We would like to thank the reviewers for their efforts in reviewing this manuscript, and we feel that the manuscript is much stronger with the suggested changes. Below are detailed responses to their comments, which are highlighted in italics.

Reviewer #1

This study focuses on the analysis of the OH and HO2* radicals concentrations and total OH reactivity during the IRRONIC field campaign. The campaign was performed in a forested area characterized by high isoprene emissions and low NO concentrations. Measured radicals, which include a possibly interference-free OH radical measurement, are compared with two mechanisms (RACM2 and MCM) both with and without isomerization reactions for isoprene-RO2 as described within the LIM1 mechanism.

The paper is well written and the data are adequately presented. Though, the analysis of the results and the discussion of the findings is too limited and in the current status this reviewer is not sure it is enough for publication on ACP. Following are some general comments which could help improving the discussion.

One of the problems of this study is the lack of NO data for a large fraction of the campaign. The authors overcome the issue by using the measured diurnal average when no NO data is available. I do not think this is a very good approach. Indeed, a much better solution is to constrain the model to the ozone and NO2 concentrations and jNO2 values and let the model calculate the NO. This is shown only for one model run (MCM 331) but should be done for all the models. Also, the modeled NO concentration should be compared with the measured one to see how well the model is able to reproduce it. This would allow for a better confidence in the models output also for days were no NO measurements are available.

*We agree that constraining the model to the measured ozone, NO2, and jNO2 and allowing the model to calculate NO is an alternative approach to addressing the lack of NO measurements in this study. However, the measurements suggest that deviations from the ozone photostationary state were significant at this site, implying that the concentrations of peroxy radicals were high enough to significantly impact the concentration of NO. In addition, the location of the site relatively close to NO sources from transportation as well as soil emissions may also impact the NO/NO2 ratio, as pointed out by Reviewer #2. For these reasons, we chose to constrain the model to the measured diurnal averaged NO to predict the radical concentrations rather than allowing the model to calculate the NO. We have clarified this in the revised manuscript on page 9:*

“*Zero-dimensional models cannot explicitly account for emissions, and NO is emitted both by vehicles on the nearby highway 1 km to the Southwest and by soil. Such local perturbations to the NOx-O3-radical chemistry necessitate using constrained measurements of NO, NO2, and O3.*"

*However, we have included additional model runs with NO calculated by the model as suggested by the reviewer. Figure 6 in the revised manuscript now includes results from the MCM 3.2*

*model in addition to the MCM3.3.1 results. For clarity, the NO unconstrained RACM2 and RACM2-LIM1 results are included in an additional plot in the Supporting Information.*

*On days when NO was measured, the modeled calculated NO overpredicted the measured NO during the day, and underpredicted it in the morning and at night, suggesting that the assumption of an NO/NO2 steady-state may not be justified. An additional plot illustrating the inability of the model to reproduce the measured NO is also included in the Supporting Information.*

*We have added the following to the revised manuscript addressing these points on page 12:*

*"However, the assumption that NO is in steady-state may not be justified given the location of the site near NO sources from transportation as well as the potential influence of soil emissions (Molina-Herrera et al., 2017). In addition, the measurements suggest that deviations from the ozone photostationary state were significant at this site, implying that the concentrations of peroxy radicals were high enough to significantly impact the concentration of NO. On the days when NO was measured, the models overpredicted the NO measurements by a factor of approximately 2-4 during the day, and underpredicted the measurements in the morning and evening (Fig. S3). This underprediction of the measured NO in the morning and evening may reflect active NO sources from soil and transportation emissions, and could explain why the NO unconstrained model underpredicts the concentration of OH in the afternoon."*


It would be good to focus on the days when the measurements are complete and try and understand why there is still a discrepancy between modeled and measured OH radicals even after the inclusion of the LIM1 mechanisms. On those days it could be good to perform an experimental budget if possible. I can understand it could be difficult as the HO2* radical measurement is affected by an interference from RO2 radicals but a % of this interference is given based on laboratory studies so it should be possible to remove it. This would allow for an additional way to assess whether there is a discrepancy between the included sources of OH radicals and the total OH radical production.

*Unfortunately there were only a few days during the campaign when the measurements were complete. As discussed in the manuscript, the models including the LIM1 are in better agreement with the measured OH and HO2* concentrations on these days, illustrating the ability of the model to reproduce the measurements when NO was measured simultaneously. For 20 July, the RACM2-LIM1 and MCM 3.3.1 models predict a maximum concentration of OH that are within 30% of the measured concentration, in better agreement than the models without the LIM1 mechanism. We have clarified this in the revised manuscript on page 12 and included an additional figure in the Supporting Information highlighting the agreement of the LIM1 models with the measurements on this day:*

*"For the days at the end of the campaign where there was significant overlap between the measurements of OH and NO, the model results are in better agreement during these days (20*

*and 24 July) (Fig. 5). On 20 July, the RACM2-LIM1 and MCM 3.3.1 models predict maximum OH concentrations that are within 30% of the measured OH on 20 July (Fig. S1).*

*As pointed out by the reviewer, an experimental budget for the days where the measurements are complete can provide some information regarding the source of discrepancies with the model. An experimental OH radical budget analysis for 20 July suggests that the measured OH production is less than total OH loss. However, including the modeled OH production from the LIM1 mechanism brings the total OH production into reasonable agreement with total OH loss on this day, with the measured OH production rates (including the modeled LIM1 contribution) within 30% of the measured OH loss rate, consistent with the ability of the LIM1 mechanisms to reproduce the maximum measured OH concentration on this day. This is discussed in the revised manuscript on page 15 and the experimental budget is included in the Supporting Material:*

*"An experimental radical budget for 20 July when the measurements were complete suggests that the total measured OH production rate is nearly balanced by the total OH loss rate calculated by the concentration of individual sinks and the loss rate based on the measured total OH reactivity to within approximately 30% (Fig. S8), consistent with the agreement between the measured and modeled OH on this day as discussed above. For simplicity, the measured HO2\* was used to calculate the rate of OH production from the HO2 + NO reaction and as a result the measured production rate represents an upper limit to the overall OH production rate. Thus, the difference between production and loss may be greater than illustrated in this figure, but is still likely to be within the combined uncertainties of all the measurements (for example 38% (2σ) for OH and for HO2), similar to that observed previously (Tan et al., 2019)."*


Both RACM2 and MCM mechanisms are used in this study but there is no discussion about why both are used and, based on the results, which one is able to better reproduce the measured data and why. As both are used extensively within the community a better analysis of the differences between the two should be given. Also, both are implemented with the LIM1 mechanism. Is this done in the same way or are there differences? What is the reason behind the large differences in the modeled HO2\* concentrations between the two mechanisms?

*As indicated by the reviewer, we chose to use both RACM and MCM mechanisms to model these results given that both are used extensively within the community. While the MCM mechanism is a more explicit mechanism expected to better reproduce complex systems, the lumped RACM mechanism provides a simpler radical budget analysis. We have clarified the reason for using these mechanisms on page 9 of the revised manuscript, in addition to clarifying how the LIM1 mechanism is incorporated in each:*

*"While the MCM model provides a near-explicit chemical mechanism and is expected to better represent complex chemical atmospheres, the lumped RACM mechanism is easier to use in radical budget calculations. The isoprene oxidation mechanism in RACM2 was updated as described in Tan et al. (2017) to include the Leuven Isoprene Mechanism (LIM1) originally proposed by Peeters, et al. (2009) involving peroxy radical isomerization reactions leading to additional HOx radical production, and includes the LIM1 updated bulk RO2 reactions*

*described in Peeters et al. (2014). The addition also includes a revision of the chemistry of first-generation isoprene oxidation products, including methyl vinyl ketone (MVK), methacrolein (MACR), and isoprene hydroperoxides (ISHP) (Tan et al., 2017). In addition, the ambient measurements were also modeled with version 3.3.1 of the Master Chemical Mechanism (MCM). In comparison to MCM 3.2, MCM 3.3.1 includes an updated isoprene oxidation mechanism based on the LIM1 mechanism resulting in HOx recycling from peroxy radical H-shift isomerization reactions (Jenkin et al., 2015)."*

*During an analysis in response to the reviewer noting the difference between the modeled HO2\* by the two mechanisms, we found a discrepancy in the model results illustrated in Figure 6. Correcting this discrepancy resulted in better agreement in the modeled HO2\*concentrations by the two mechanisms, with predicted maximum concentrations agreeing to within 10%. This has been clarified in the revised manuscript and the corresponding figures and discussion has been updated.*

The total OH reactivity measurement shows that, overall, when the contribution from modelled OVOCs is included, the budget is closed. Though, this is not true for some days when still a certain fraction of OH reactivity is unexplained. It would be good to look if there were differences between these days and the ones were the OH reactivity could be explained…different wind directions, different VOCs distribution, different meteorological conditions, etc. Does this missing reactivity correlate with the days where the measured OH concentration is larger than the modelled one?

*We have done an extensive analysis of the missing reactivity measured during this campaign, including analyzing different wind directions, velocity, trajectories, meteorological conditions, etc. and have yet to find an explanation for the missing reactivity. We are continuing this analysis and plan to do additional measurements in the future. This has been clarified on page 15 of the revised manuscript:*

*"The reason for this discrepancy is unclear, as the missing reactivity on this day did not appear to correlate with changes in wind speed, direction, trajectory, or meteorological conditions, but may indicate the presence of additional unmeasured emissions or oxidation products not accounted for by the model. Additional measurements and analyses will be necessary to determine the source of the missing reactivity."*

In general, often it is written the agreement is good or there is better agreement… but there is no value reported of a ratio of model to measurement or correlation coefficient so it is not possible to really assess the correctness of these statements.

*We have attempted to include more quantifiable comparisons in the revised manuscript as suggested.*

Specific comments:

Abstract: It would be good to have, in addition to percentages, also the mean concentrations of radicals and OH reactivity and what low NOx means.

*These suggestions have been added to the abstract.*

Page 2, Line 12 to 17. No mention of the recent campaigns performed in China (Tan et al., 2017; Tan et al., 2018; Tan et al., 2019).

*We have added these references as suggested.*

Page 5, Line 11. Is it pure NO injected to convert HO2 to OH radicals? Or why is the interference from RO2 radicals so large? Would not it make sense to reduce the NO further to reduce the interference?

*One of the goals of this study was an instrumental intercomparison of peroxy radical measurements by the IU-FAGE instrument with the HO2+RO2 measurements by the Drexel University Ethane – Nitric Oxide Chemical Amplifier (ECHAMP) instrument. In order to provide a useful intercomparison, high concentrations of NO (10% in N2) were deliberately added to the IU-FAGE instrument to allow for efficient conversion of isoprene peroxy radicals in addition to HO2. Given that the total peroxy radical concentrations at this site were primarily HO2 and isoprene peroxy radicals, the resulting HO2\* measurements were found to be similar to the total HO2+RO2 measurements by the ECHAMP instrument. The results of this intercomparison are summarized in a separate publication (Kundu et al., 2019). This has been clarified on page 7 of the revised manuscript:*

*"A high concentration of NO leading to a high conversion efficiency of isoprene-based peroxy radicals to HO2 was used throughout the study to provide a useful intercomparison of the IU-FAGE HO2\* measurements with the RO2+HO2 measurements by the Drexel University Ethane – Nitric Oxide Chemical Amplifier (ECHAMP) instrument (Kundu et al., 2019), as HO2 and isoprene-based peroxy radicals accounted for approximately 70% of the total peroxy radicals at this site (see below)."*

Page 9, Line 1. Is the LIM or the LIM1 included in both RACM2 and MCM 3.3.1?

*The updated RACM2 mechanism (RACM2-LIM1) described in Tan et al. (2017) includes updates to the LIM rates as described in Peeters et al., 2014. This has been clarified in the revised manuscript. The MCM 3.3.1 mechanism also includes the updated LIM1 mechanism as described in Jenkin et al., (2015) and this has been clarified in the revised manuscript, as noted above.*

Page 10, Line 34. What does it mean that measurements on the 21-22 July focused on the HO2* thus OH measurements were not available? The instrument should measure OH and HO2 radicals in parallel or? How is stopping the OH measurement going to improve the measurement of HO2* radicals?

*The IU-FAGE instrument is composed of a single detection axis for measuring both OH and HO2, and as a result cannot measure OH and HO2 simultaneously. This has been clarified on page 4 of the revised manuscript:*

*"The Indiana University LIF-FAGE instrument (IU-FAGE) has been described in detail previously and consists of a single axis for alternating measurements of OH and HO2 or HO2* (Dusanter et al., 2009a Griffith et al., 2013; 2016)."*

*For most of the campaign, NO was added for 30 seconds every 30 minutes to measure HO2*, while OH was measured during the remaining time. As part of the peroxy radical intercomparison with the Drexel University ECHAMP instrument, NO was added continuously on 21-22 July to allow for higher time resolved measurements of HO2*. Because NO was added continuously during this time, no OH measurements were made on these days. This has been clarified on page 11 of the revised manuscript:*

*"Measurements on 21-22 July focused on measurements of HO2* as part of the peroxy radical informal instrumental intercomparison (Kundu et al., 2019), with NO added continuously to the detection cell to provide measurements with a higher time resolution. Thus OH measurements were not conducted on these days."*

Page 16, Line 9. What does "similar OH" stands for?

*This has been revised to* *"similar concentrations of OH have been observed at this site…"*

Figure 5. Colors of the models are different between OH and HO2* panels.

*We have corrected the panels so that the color of the model results are consistent.*

Figure 12. Suggest to have consistency of the colors within the upper and lower panels.

*We have revised the colors as suggested.*

We would like to thank the reviewers for their efforts in reviewing this manuscript, and we feel that the manuscript is much stronger with the suggested changes. Below are detailed responses to their comments, which are highlighted in italics.

Reviewer #2

The paper describes measurements of OH reactivity, OH and HO2* in a biogenic dominated regime with medium NO concentrations during daytime in the order of a few hundred pptv and compares the measurements with a box model study using four different model schemes. The main findings are that the model describes well the measured HO2* but underestimates the OH concentration. The most likely reason identified is a poor quality of the available NO measurements for the time periode shown. When the model is constrained by NO2 to calculate the NO concentration a better agreement of the model is found but local NO sources, independent of the photolysis of NO2 worsen the agreement as soon as the steady state assumption cannot be made anymore. The paper also shows that the Indiana instrument successfully implemented a chemical scavenging modulation, improving the quality of the OH measurements. The quality of the dataset does not allow a detailed investigation of testing different model schemes, though it is obvious that the LIM1 based recycling reactions do provide a better agreement in the late afternoon when Isoprene is larger. The paper is well written, hPa seems to me preferable than Torr. The paper can be published after minor corrections.

P3 L11 : The statement "The extent of RO2 radical contributions during HO2 measurements in previous campaigns is unclear." Is not correct. For HUMPPA 2010 the contribution of a RO2 interference to the HO2* signal had been estimated based on H2O2 in Hens et al 2014, as well as calculated based on the PAA-PAN-HO2 system in Crowley et al. 2018 . Mallik et al. 2017 did model the internal production of OH from RO2 as well as compared it with a NO titration scheme done routinely in ambient air during the CYPHEX 2014 campaign.

*We have clarified on page 3 of the revised manuscript that while there are several campaigns where the extent of any RO2 interference on the HO2 measurements has been estimated and accounted for (and have included the noted references in the revised manuscript), there are many previous studies which the contribution of a RO2 interference in the HO2 measurements is not known:*

*"The degree to which the RO2 species can interfere with HO2 measurements has been quantified through several laboratory experiments (Fuchs et al., 2011; Whalley et al., 2013; Lew et al., 2018) and estimated in some field studies (Hens et al., 2014; Crowley et al., 2018; Mallik et al., 2018). However, the extent of RO2 radical contributions during HO2 measurements in many of the campaigns mentioned above is unclear."*

P4 L29 : To what extend is double pulsing an issue, considering the volume flow, the expansion of the UV beam due to the white cell and the 10kHz repetition rate?

*The instrument design and configuration is similar to that described in Stevens et al. (1994). The flow velocity in the region of the White cell is likely greater than the 50 m s-1 required to prevent double-pulsing of the air stream. However, any laser-generated OH is measured and accounted for through the interference measurements.*

P4 L29 : please use SI units

*We have converted to SI units as requested.*

P6 L28 : Unclear why the precision of the HO2* measurements is unrelated to the RO2 interference. Why would not the variability in the relative RO2 & HO2 composition translate into a variability in HO2* and therefore in an apparent precision?

*We have clarified on page 7 of the revised manuscript that the instrumental precision of the measurements is primarily related to the variation in the background signal due to laser scatter and detector noise in the detection cell:*

*"The instrumental precision for the HO2* measurement based on the variability of the background signal due to laser scatter and detector noise results in a limit of detection for HO2* during this campaign of 7 × 107 cm-3 for a 30 second average (S/N =1)."*

P8 L18: Please be more specific why a constant scaling factor can be used. Hansen et al. 2014 does not describe further the reason for the factor 1.4 beyond speculating about incomplete mixing or issues with the flow speed. Without knowing the fundamental reason for the factor, the application of such seems to be arbitrary.

*The constant scaling factor is derived from reproducible OH reactivity measurements in the laboratory of a variety of compounds, including butane, isoprene, and propane, which were all found to be a factor of 1.4 lower than the calculated reactivity. This has been clarified on page 8 of the revised manuscript:*

*"Laboratory measurements of the reactivity of several VOCs with well-known rate constants, including butane, isoprene, and propane showed that the OH reactivity measurements for these compounds were on average 30% lower than calculated when the measured velocity of the turbulent core is used to determine the reaction time. This consistent underestimation of the OH reactivity is likely due to either incomplete mixing of the reactants or a systematic underestimation of the reaction time (Hansen et al, 2014)."*

P9 L27: Not conclusive is a 50% contribution of the background signal between 8:00 and 20:00. In the figure it seems rather in the range of 20%-300% even just for noontime. In any case I am not sure if the fractional description is of much use anyhow as the relationship between ambient OH and chemical background OH is not clear at best. I would drop the discussion about the

fractional contribution. You mention it above already that you are using a chemical scavenger method to remove ambient OH for quantification of the non-ambient OH.

*We have removed this discussion as suggested.*

P10 L5: Do you observe a correlation of the internal background signal with O3*BVOC as described in Novelli 2017?

*The unknown interference was found to increase with the product of ozone and BVOC concentrations, similar to that found in Novelli et al., 2017, although the correlation was not statistically significant. This has been clarified on page 10 of the revised manuscript:*

*"This result is also consistent with the measurements of Novelli et al. (2017), who found that their observed interference correlated with the product of ozone and biogenic VOC concentrations, although the correlation in the present study was not statistically significant."*

P10 L12: Novelli 2014 proposed the presence sCI decomposition as reason for the internal OH.

*We have added this reference as suggested.*

P11 L4: What is the time periode used for calculating the average? Did you model the non averaged time series and then average the model together with the measurements?

*For the diurnal average shown in Fig. 6, the 15-min OH measurements with and without the interference were averaged into 1 hour bins. This has been clarified in the revised manuscript. The model results in this figure represent a model constrained by the diurnal average of the daily measurement shown in in Fig. 2, and is similar to the diurnal average of the model results. However, we did find a discrepancy in the model results previously illustrated in Figure 6. This has been corrected in the revised manuscript, and all the relevant figures have been updated.*

P11 L14: "However, as seen in Fig. 6, . . ." sentence seems to be reduntant to "If the measured interference was not subtracted from the total OH. . .."

*We have removed this sentence as suggested.*

P11 L27: Is there a NO source close by and to what extend is the assumption of steady state NO/NO2 justified? The floating NO leads to much better model estimates for OH, but seems to deviate as soon as the sun sets. From a model point of view, NO production in the model will follow JNO2, which decay quickly into the night and reduce the OH source from HO2+NO

whereas the measured OH is significant different from 0, therefore the question, is there a still active NO source close by?

*As pointed out by the reviewer, the models tend to underpredict the measured nighttime NO, suggesting that the site may be influenced by transportation by the nearby highway or perhaps more importantly local emissions of NO from soil. These active NO source likely impact the measured OH concentration and could explain the discrepancy between the measured and modeled OH concentrations in the late afternoon and early evening. This has been clarified on page 12 of the revised manuscript:*

*"However, the assumption that NO is in steady-state may not be justified given the location of the site near NO sources from transportation as well as the potential influence of soil emissions (Molina-Herrera et al., 2017). In addition, the measurements suggest that deviations from the ozone photostationary state were significant at this site, implying that the concentrations of peroxy radicals were high enough to significantly impact the concentration of NO. On the days when NO was measured, the models overpredicted the NO measurements by a factor of approximately 2-4 during the day, and underpredicted the measurements in the morning and evening (Fig. S3). This underprediction of the measured NO in the morning and evening may reflect active NO sources from soil and transportation emissions, and could explain why the NO unconstrained model underpredicts the concentration of OH in the afternoon."*


P11 & P16 Check spelling of the name, Rohrer

*This typo has been corrected.*


P 16 L25: Mallik et al, 2017 like Mao found a decent agreement of modeled OH and measured OH only when the interference, determined by a chemical modulation technique had been taken into account. I would be careful with a generalization, the instrument by the Leeds and Juelich group seem to be not as much as sensitive to the interference as the PennState/Indiana/Mainz & Lile group. The most striking difference is the use of a multipass cell vs. single beam cell.

*We have included the Mallik et al., 2017 reference as suggested. We agree that the observed interference may not be similar for all instruments, and have revised the statement accordingly on page 17 of the revised manuscript:*

*"However, it is clear that if the measured interference was not taken into account, the apparent OH concentrations would have been a factor of 5 greater than predicted by the model mechanisms, comparable to previous measurements under low NOx and high isoprene conditions (Rhorer et al., 2014). These results are similar to that reported by Mao et al. (2012) and Mallik et al. (2017) who found good agreement between their OH measurements and model predictions when measured interferences were taken into account. However, because of differences in instrument design (geometry, cell pressure, flow, etc.) these interferences may not significantly impact other LIF-FAGE instruments. However, future OH measurements using the*

*LIF-FAGE technique should include methods to quantify potential instrumental artifacts even if they are insignificant, to demonstrate that the measurements are free from interferences."*

# OH and HO₂ radical chemistry in a midlatitude forest: Measurements and model comparisons

Michelle M. Lew[1*], Pamela S. Rickly[2**], Brandon P. Bottorff[1], Emily Reidy[1], Sofia Sklaveniti[2,3], Thierry Léonardis[3], Nadine Locoge[3], Sebastien Dusanter[3], Shuvashish Kundu[4***], Ezra Wood[5], and Philip S. Stevens[1,2]

[1] Department of Chemistry, Indiana University, Bloomington, IN 47405, USA
[2] O'Neill School of Public and Environmental Affairs, Indiana University, Bloomington, IN 47405, USA
[3] IMT Lille Douai, Univ. Lille, SAGE – Département Sciences de l'Atmosphère et Génie de l'Environnement, 59000 Lille, France
[4] Department of Chemistry, University of Massachusetts - Amherst, Amherst, MA 01003, USA
[5] Department of Chemistry, Drexel University, Philadelphia, PA 19104, USA

* now at California Air Resources Board, Sacramento, CA 95812, USA
** now at Cooperative Institute for Research in Environmental Sciences, University of Colorado, Boulder, CO 80309, USA and Chemical Sciences Division, Earth System Research Laboratory, National Oceanic and Atmospheric Administration, Boulder, CO 80305, USA
*** now at Momentive Performance Materials, Inc., Tarrytown, NY 10591, United States

*Correspondence*: Philip S. Stevens (pstevens@indiana.edu)

**Abstract.** Reactions of the hydroxyl (OH) and peroxy radicals (HO₂ and RO₂) play a central role in the chemistry of the atmosphere. In addition to controlling the lifetimes of many trace gases important to issues of global climate change, OH radical reactions initiate the oxidation of volatile organic compounds (VOCs) which can lead to the production of ozone and secondary organic aerosols in the atmosphere. Previous measurements of these radicals in forest environments characterized by high mixing ratios of isoprene and low mixing ratios of nitrogen oxides (NOₓ) (typically less than 1-2 ppb) have shown serious discrepancies with modeled concentrations. These results bring into question our understanding of the atmospheric chemistry of isoprene and other biogenic VOCs under low NOₓ conditions.

During the summer of 2015, OH and HO₂ radical concentrations as well as total OH reactivity were measured using Laser-Induced Fluorescence - Fluorescence Assay by Gas Expansion (LIF-FAGE) techniques as part of the Indiana Radical, Reactivity and Ozone Production Intercomparison (IRRONIC). This campaign took place in a forested area near the Indiana University, Bloomington campus characterized by high mixing ratios of isoprene and low mixing ratios of NOₓ. Supporting measurements of photolysis rates, VOCs, NOₓ, and other species were used to constrain a zero-dimensional box model based on the Regional Atmospheric Chemistry Mechanism (RACM2) and the Master Chemical Mechanism (MCM). Using an OH chemical scavenger technique, the study revealed the presence of an interference with the LIF-FAGE measurements of OH that increased with both ambient concentrations of ozone and temperature. Subtraction of the interference resulted in measured OH concentrations (approximately $4 \times 10^6$ cm⁻³ average daytime maximum) that were in better agreement with model

1

predictions, although the model still underestimated the measured concentrations, likely due to an underestimation of the concentration of NO at this site. Measurements of $HO_2$ concentrations during the campaign (approximately $1 \times 10^9$ cm$^{-3}$ average daytime maximum) included a fraction of isoprene-based peroxy radicals ($HO_2^* = HO_2 + \alpha RO_2$) and were found to agree with model predictions to within 20%. On average, the measured reactivity was consistent with that calculated from measured OH sinks to within 20%, with modeled oxidation products accounting for the missing reactivity, although significant missing reactivity (approximately 40% of the total measured reactivity) was observed on some days.

**1 Introduction**

The hydroxyl radical (OH) is one of the primary oxidants in the atmosphere (Levy, 1972). The OH radical initiates the oxidation of volatile organic compounds (VOCs) that leads to the production of hydroperoxy radicals ($HO_2$) and organic peroxy radicals ($RO_2$). In the presence of nitrogen oxides ($NO_x = NO + NO_2$), reactions of these radicals can lead to the production of ozone and secondary organic aerosols in the atmosphere, the primary components of photochemical smog. Because of their short atmospheric lifetimes, measurements of OH and $HO_2$ (together $HO_x$) and total OH reactivity can provide a robust test of our understanding of this complex chemistry (Heard and Pilling, 2003).

Multiple field campaigns have been conducted over the years measuring OH and $HO_2$ radicals in both urban and forested environments. Measurements of OH in urban areas characterized by high mixing ratios of $NO_x$ and anthropogenic VOCs have been generally consistent with model predictions (Ren et al., 2003; Shirley et al., 2006; Kanaya et al., 2007a; Dusanter et al., 2009b; Hofzumahaus et al., 2009; Griffith et al., 2016; Tan et al., 2017; 2018; 2019), while measurements in remote forested environments characterized by low mixing ratios of $NO_x$ and high mixing ratios of biogenic VOCs have often been greater than model predictions (Tan et al., 2001; Lelieveld et al., 2008; Whalley et al., 2011; Rohrer et al., 2014).

However, recent measurements by Mao et al. (2012) in a northern California forest using a new chemical scavenging technique that removes ambient OH before air enters the detection cell revealed a significant interference associated with their Laser-Induced Fluorescence (LIF) measurements of OH. The unknown interference was a factor of 2 to 3 times higher than ambient OH concentrations (Mao et al., 2012). Similar results were observed in a boreal forest by Novelli et al. (2014), who observed an interference using a similar chemical scrubbing technique that was a factor of 3 to 4 times higher than ambient OH concentrations. One possible source of this observed interference may be the decomposition of Criegee intermediates produced from the ozonolysis of biogenic emissions in the low-pressure detection cells used by LIF instruments, although the ambient concentration of these intermediates in the atmosphere may be too low to explain all of the observed interference (Novelli et al., 2017; Rickly and Stevens, 2018). Another proposed source of the interference is the decomposition of ROOOH molecules inside the FAGE detection cell formed from the reaction of OH with $RO_2$ radicals (Fittschen et al., 2019). Nevertheless, interferences associated with measurements of OH could explain part of the discrepancies between measured and modeled OH concentrations in forested environments. Monitoring potential interferences associated with OH measurements using LIF techniques may be crucial for understanding the discrepancies between measurements and models.

1    In contrast to measurements of OH, the agreement between measured and modeled $HO_2$ concentrations have been
2    highly variable. In urban environments, measured $HO_2$ concentrations were sometimes found to agree with model predictions
3    (Shirley et al., 2006; Emmerson et al., 2007; Dusanter et al., 2009b; Michoud et al., 2012; Lu et al., 2013; Ren et al., 2013;
4    Griffith et al., 2016; Tan et al., 2017), while other times the measurements were found to be both lower (George et al., 1999;
5    Konrad et al., 2003) and higher than model predictions (Martinez et al., 2003; Ren et al., 2003; Emmerson et al., 2005; Kanaya
6    et al., 2007a; Chen et al., 2010; Sheehy et al., 2010; Czader et al., 2013; Griffith et al., 2016; Tan et al., 2018). In forested
7    environments, measured $HO_2$ concentrations were sometimes found to agree with model predictions (Tan, D. et al., 2001; Ren
8    et al., 2005; 2006), but were often found to be either lower (Carslaw et al., 2001; Kanaya et al., 2007b; Whalley et al., 2011;
9    Kanaya et al., 2012; Mao et al., 2012; Griffith et al., 2013; Mallik et al., 2018), or higher than model predictions (Carslaw et
10   al., 2001; Kubistin et al., 2010; Kim et al., 2013; Hens et al., 2014). Part of this variability may be due to interferences from
11   alkene and aromatic based $RO_2$ radicals converting to $HO_2$ in systems that detect $HO_2$ through conversion to OH by addition
12   of NO in the sample cell. The degree to which the $RO_2$ species can interfere with $HO_2$ measurements has been quantified
13   through several laboratory experiments (Fuchs et al., 2011; Whalley et al., 2013; Lew et al., 2018) and estimated in some field
14   studies (Hens et al., 2014; Crowley et al., 2018; Mallik et al., 2018). However, the extent of $RO_2$ radical contributions during
15   $HO_2$ measurements in many of the campaigns mentioned above is unclear.
16       Total OH reactivity measurements can complement $HO_x$ measurements by providing a constraint on the total loss of
17   OH that can be compared to that calculated from co-located measurements of OH sinks. Several recent studies have identified
18   discrepancies between measured and calculated OH reactivity in which the measured values are significantly greater than the
19   calculated values (Di Carlo et al., 2004; Hansen et al., 2014; Nölscher et al., 2016; Zannoni et al., 2016). This difference has
20   been attributed to OH loss from unmeasured VOCs and their oxidation products. In general, significant missing OH reactivity
21   has not been observed as often in urban environments as it has in forested areas, bringing into question our understanding of
22   the chemistry of biogenic emissions and their oxidation products (Dusanter and Stevens, 2017).
23       This study reports measurements and model simulations of $HO_x$ radical chemistry as well as OH reactivity for a
24   forested site located in Bloomington, Indiana during the 2015 IRRONIC (Indiana Radical Reactivity and Ozone productioN
25   InterComparison) field campaign. This work compares the measured $HO_x$ radical concentrations to model predictions
26   incorporating the Regional Atmospheric Chemistry Mechanism 2 (RACM2), in addition to a version updated to include the
27   Leuven Isoprene Mechanism (RACM2-LIM1), as well as the Master Chemical Mechanism versions 3.2 and 3.3.1 in order to
28   test the ability of each model to reproduce the observed radical concentrations and total OH reactivity.

29   **2 Experimental section**

30   **2.1 IRRONIC location and supporting measurements**

31   The IRRONIC campaign site was located within a mixed deciduous forest (sugar maple, sycamore, tulip polar, ash and hickory
32   trees) at the Indiana University Research and Teaching Preserve (IU-RTP) field lab (39.1908º N, 86.502º W) located

approximately 2.5 km northeast of the center of the Indiana University campus, and 1 km from the IN 45/46 bypass at the northern perimeter. The goals of the campaign included an informal intercomparison of peroxy radical measurements by two different techniques (Kundu et al., 2019), an analysis of ozone production sensitivity at this site (Sklaveniti et al., 2018), a comparison of measured OH radical reactivity with that calculated from measured VOCs, and a comparison of measured OH, $HO_2$, and $RO_2$ radicals with model predictions. The main biogenic emission within this area was isoprene, with an average daytime maximum mixing ratio of approximately 4 ppb during the campaign. This area exhibited low anthropogenic influence from the campus area, with an average daytime maximum mixing ratio of NO of approximately 315 ppt and an average daytime maximum $NO_2$ mixing ratio of approximately 2 ppb. Measurements were conducted on top of two scaffolding platforms adjacent to the field lab, approximately 1.8 m from the ground. Additional information regarding the field site and the IRRONIC campaign can be found in Sklaveniti et al. (2018) and Kundu et al. (2019).

Table 1 summarizes the major instrumentation employed during the campaign. NO was measured every 10 s using a chemiluminescence instrument (Thermo model 42i-TL, detection limit 50 ppt / 2 min). Periodic problems with the sensor's high voltage power supply that required an eventual replacement limited the coverage of the measurements. $NO_2$ was measured every 1 s by a Cavity Attenuated Phase Shift (CAPS) instrument (detection limit 40 ppt / 10 s), and ozone was measured every 10 sec using a 2B Technologies model 202 UV absorbance instrument (detection limit 3 ppb / 10 s). Further details on the calibration and baseline measurements for the NO, $NO_2$, and $O_3$ measurements are described in Kundu et al. (2019). Nonmethane hydrocarbons, including C2-C10 alkanes and alkenes, butadiene, C6-C9 aromatic compounds, isoprene, α-pinene, and β-pinene, were measured using a thermal desorption GC/FID instrument with a 1.5-h time resolution. Oxygenated VOCs (OVOCs), including C2-C10 aldehydes, C2-C6 ketones, and C2-C4 alcohols, were measured by thermal desorption GC/FID-MS with a 1.5-h time resolution. Offline sampling focused on measurements of oxygenated VOCs including formaldehyde and C2-C6 aldehydes, acetone, MEK, glyoxal and methylglyoxal using DNPH cartridges and HPLC-UV analysis. C6-C16 VOCs including α-pinene, β-pinene, limonene, camphene, heptane-hexadecane, methylpentene-pentadecene were measured using Sorbent cartridges and GC-MS analysis. Measurements of J($NO_2$) were made by spectral radiometry courtesy of the University of Houston. HONO was measured using a newly developed Laser Photofragmentation/Laser-Induced Fluorescence instrument (Bottorff et al., 2015; manuscript in preparation).

## 2.2 HOx radical measurements

The Indiana University LIF-FAGE instrument (IU-FAGE) has been described in detail previously and consists of a single axis for alternating measurements of OH and $HO_2$ or $HO_2$* (Dusanter et al., 2009a Griffith et al., 2013; 2016). In the LIF-FAGE technique, OH radicals are detected by laser-induced fluorescence after expansion of ambient air to low pressure. This extends the OH fluorescence lifetime, allowing temporal filtering of the fluorescence from laser scatter (Heard and Pilling, 2003). Ambient air is expanded through a 0.64 mm diameter orifice located at the top of a cylindrical nozzle (5 cm in diameter and 20 cm long), resulting in a flow rate of approximately 3 SLPM through the sampling nozzle. Two scroll pumps (Edwards XDS 35i) connected in parallel maintain a pressure inside the cell of 7.3 hPa.

The laser system used in this study consisted of a Spectra Physics Navigator II YHP40-532Q that produces approximately 8 W of radiation at 532 nm at a repetition rate of 10 kHz which is used to pump a Sirah Credo Dye laser (255 mg/L of Rhodamine 610 and 80 mg/L of Rhodamine 101 in ethanol), resulting in 40 to 100 mW of radiation at 308 nm. After exiting the dye laser, a fraction of the radiation is focused onto the entrance of a 12-m optical fiber to transmit the radiation to the sampling cell which was placed on top of the 1.8-m platform adjacent to the field lab. In the detection cell, the laser crosses the expanded air perpendicular to the flow in a White cell configuration with 24 passes. For this campaign, the laser power inside the sampling cell ranged from 0.5 to 4.4 mW and was monitored using a photodiode at the exit of the White cell.

OH radicals are excited and detected using the $A^2\Sigma^+$ $v' = 0 \leftarrow X^2\Pi$ $v'' = 0$ transition near 308 nm (Stevens et al., 1994). The net signal is measured by spectral modulation by tuning the wavelength on- and off-resonance in successive modulation cycles. A reference cell where OH is produced by thermal dissociation of water vapor is used to ensure that the laser is tuned on and off the OH transition. The OH fluorescence is detected using a microchannel plate photomultiplier tube (MCP-PMT) detector (Hamamatsu R5946U-50), a preamplifier (Stanford Research System SR445) and a gated photon counter (Stanford Research Systems SR 400). The MCP-PMT is switched off during the laser pulse through the use of electronic gating allowing the OH fluorescence to be temporally filtered from laser scattered light. A Teflon injector located approximately 2.5 cm below the inlet and 17.5 cm above the detection axis allowed for the addition of NO (approximately 2 sccm, $1.4 \times 10^{13}$ cm$^{-3}$, Matheson Gas, 10% in N$_2$) to convert ambient HO$_2$ to OH through the fast HO$_2$ + NO $\rightarrow$ OH + NO$_2$ reaction, allowing for indirect measurements of HO$_2$.

The IU-FAGE instrument is calibrated by producing known quantities of OH and HO$_2$ from the photolysis of water vapor in air using a mercury penlamp within the calibration source as described previously (Dusanter et al., 2008). For these calibrations, zero air was sent through a humidifier and delivered at a flow rate of 38-50 L min$^{-1}$ to the calibration source. Uncertainties associated with the UV water photolysis calibration technique have been described previously (Dusanter et al., 2008) and are estimated to be 18% (1$\sigma$) for both OH and HO$_2$.

### 2.2.1 Measurement of OH interferences

The LIF-FAGE measurements are subject to potential interferences where OH radicals are generated inside the detection cell. For example, ozone can be photolyzed by the laser and in the presence of water vapor can produce hydroxyl radicals (Davis et al., 1981a; 1981b) (reactions R1 and R2):

$$O_3 + hv \rightarrow O(^1D) + O_2 \qquad\qquad (R1)$$
$$O(^1D) + H_2O \rightarrow 2OH \qquad\qquad (R2)$$

This interference in the IU-FAGE instrument is monitored through laboratory calibrations utilizing various concentrations of ozone, water vapor, and laser power. To characterize this and any other interference during ambient measurements, a chemical scrubbing technique is used to remove ambient OH prior to entering the detection cell (Griffith et al., 2016; Rickly and Stevens, 2018). This chemical modulation technique is used to monitor levels of the laser-generated ozone-water interference and any other processes that may produce OH radicals within the excitation axis.

Hexafluoropropylene ($C_3F_6$, 95.5% in $N_2$, Matheson) is added through a circular injector 1 cm above the nozzle with a flow rate of approximately 3.5 sccm to remove 95% of externally generated OH (Rickly and Stevens, 2018). During ambient measurements, chemical addition of $C_3F_6$ is modulated in between ambient OH measurements every 15 minutes for a duration of 10 minutes. The differences between the measured OH during $C_3F_6$ addition and OH measurements including the interference represents the net ambient OH concentration in the atmosphere. Taking the measurement of potential interferences into account results in a limit of detection for OH for this campaign of approximately $7.9 \times 10^5$ $cm^{-3}$ for a 30 min average (S/N = 1).

**2.2.2 Contribution of RO$_2$ interferences during HO$_2$ measurements**

As discussed above, HO$_2$ radicals are measured indirectly after sampling ambient air at low pressure through chemical conversion to OH by addition of NO and subsequent detection of OH by LIF:

$$HO_2 + NO \rightarrow OH + NO_2 \qquad\qquad (R3)$$

It was previously believed that the detection of HO$_2$ radicals using this technique was free from interferences from the reaction of RO$_2$ radicals with NO, as model simulations and measurements suggested that the rate of conversion of RO$_2$ radicals to HO$_2$ by reactions R4 and R5 and subsequent conversion to OH through reaction R3 were negligible. This was due to the slow rate of reaction R5 under the reduced oxygen concentration in the low pressure LIF-FAGE cell and the short reaction time between injection of NO and detection of OH (Heard and Pilling, 2003).

$$RO_2 + NO \rightarrow RO + NO_2 \qquad\qquad (R4)$$

$$RO + O_2 \rightarrow R'O + HO_2 \qquad\qquad (R5)$$

For example, RO$_2$ radicals produced from the OH-initiated oxidation of small alkanes were found to produce a negligible yield of HO$_2$ (Stevens et al., 1994; Kanaya et al., 2001; Tan, et al., 2001; Creasey et al., 2002; Holland et al., 2003). However, recent laboratory studies have shown that there are interferences associated with measurements of HO$_2$ from the conversion of RO$_2$ radicals derived from the OH-initiated oxidation of alkenes and aromatics to HO$_2$ (and subsequently OH) by reaction with NO. The high conversion efficiency of alkene-based peroxy radicals to HO$_2$ is due to the ability of the β-hydroxyalkoxy radicals produced from OH + VOC reactions to rapidly decompose, forming a hydroxyalkyl radical which then reacts rapidly with O$_2$ leading to the production of a carbonyl compound and HO$_2$ (Fuchs et al., 2011; Whalley et al., 2013; Lew et al., 2018). Because of this interference, measurements of peroxy radicals that are sensitive to this interference are denoted as HO$_2$* ([HO$_2$*] = [HO$_2$] + α [RO$_2$], 0<α<1). The conversion efficiency depends on the instrumental characteristics and configurations employed as well as the amount of NO added. The RO$_2$-to-HO$_2$ conversion efficiencies for a number of different peroxy radicals have been characterized for current and past configurations of the IU-FAGE instrument (Lew et al., 2018). For the configuration of the IU-FAGE instrument used in this study, the conversion efficiency of isoprene-based peroxy radicals was found to be approximately 83%, while the conversion efficiency of propane peroxy radicals was found to be

approximately 15%. A high concentration of NO leading to a high conversion efficiency of isoprene-based peroxy radicals to $HO_2$ was used throughout the study to provide a useful intercomparison of the IU-FAGE $HO_2$* measurements with the $RO_2$+$HO_2$ measurements by the Drexel University Ethane – Nitric Oxide Chemical Amplifier (ECHAMP) instrument (Kundu et al., 2019), as $HO_2$ and isoprene-based peroxy radicals accounted for approximately 70% of the total peroxy radicals at this site (see below). The instrumental precision for the $HO_2$* measurement based on the variability of the background signal due to laser scatter and detector noise results in a limit of detection for $HO_2$* during this campaign of $7 \times 10^7$ $cm^{-3}$ for a 30 second average (S/N =1).

**2.3 OH reactivity measurements**

The IU Total OH Loss rate Method (TOHLM) instrument is based on the method of Kovacs and Brune (2001) and is described in detail elsewhere (Hansen et al., 2014). Briefly, the instrument is comprised of a flow tube reactor measuring 5 cm in diameter and 75 cm in length. Ambient air is introduced through an 8 cm diameter perfluoroalkoxy polymer film hose attached to the flow tube at a flow rate of approximately 180 SLPM using a regenerative blower (Spencer VB001) to establish turbulent flow conditions. Previous measurements have demonstrated that different lengths of this inlet tubing do not significantly impact the measured OH reactivity (Hansen et al., 2014). A pitot-static tube (Dwyer Instruments) is positioned just before the exit of the flow tube facing the turbulent core of the flow, approximately 1 cm from the flow tube wall. The pitot-static tube is connected to a differential pressure gauge (MKS Instruments) to measure the total flow tube velocity.

OH radicals are produced in a movable injector that houses a mercury pen lamp (UV Pen-Ray) in which the top of the pen lamp was positioned at the end of the injector, just before a spiral Teflon spray nozzle used to promote mixing within the flow tube (McMaster Carr). In addition, a turbulizer is attached to the injector tube 24 cm before the spray nozzle consisting of four 1 cm wide fins to promote turbulent flow conditions as well as to provide support of the injector throughout the flow tube. The injector is inserted along the main axis and is configured for automated movement acquiring continuous measurements in the forward and backward directions. A nitrogen flow of 10 standard liters per minute (SLPM) is bubbled through high-purity water (EMD Chemicals) producing water vapor which is directed through the injector and photolyzed by the penlamp to produce OH with typical concentrations on the order of $10^9$ $cm^{-3}$. This method is known to also produce $HO_2$ radicals, which can lead to a regeneration of OH at NO mixing ratios greater than 1 ppbv (Kovacs and Brune, 2001). However, because the average NO mixing ratio measured over the course of the campaign was below this value, no correction to the measured reactivity was applied (Hansen et al., 2014).

OH radicals were measured using a similar FAGE detection cell described above. Ambient air was expanded through a 1 mm diameter orifice to a total pressure of approximately 8 hPa. OH radicals were excited by a portion of the 308 nm output of the dye laser, with the resulting fluorescence detected by a gated channel photomultiplier tube detector (Excelitas MP 1300) and monitored by a photon counter (Stanford Research SRS 400). A 2 meter long optical fiber was used to transmit the 308-

nm laser beam to the OH reactivity detection cell which was located inside the field lab. The laser power was measured at the exit of the detection cell and monitored with a photodiode.

As ambient air entered the flow tube, the automated OH source injector allowed for varying reaction time with the ambient air over a distance of approximately 15 cm for a period of 2.5 minutes. This produced an OH decay over a reaction time of 0-0.15 s from which the OH reactivity was determined. Losses of OH on the walls of the flow tube were measured by flowing high-purity nitrogen (Indiana Oxygen) at 180 SLPM through the flow tube in addition to the OH production through the injector to measure the decay of OH in the absence of any VOCs. Several measurements of this wall loss ($k_b$) resulted in an average value of $10 \pm 2$ s$^{-1}$ ($1\sigma$).

The calculated OH reactivity for a measured compound X ($k_X$), can be determined from the product of the concentration of X and its second-order rate constant with OH:

$$k_X = k_{OH+X}[X] \tag{1}$$

Summation of this value for each reacting species gives the total OH reactivity ($k_{OH}$):

$$k_{OH} = \sum_i k_{OH+X_i}[X_i] \tag{2}$$

Under pseudo-first order conditions ([OH]<<[X]), the OH concentration within the flow tube can be expressed as a first-order exponential decay:

$$[OH]_t = [OH]_0 e^{-(k_{OH}+k_b)t} \tag{3}$$

Solving for $k_{OH}$, the OH reactivity, gives:

$$k_{OH} = -\frac{\Delta \ln[OH]}{\Delta t} - k_b \tag{4}$$

Measurements of the change in the concentration of OH over the reaction time produces the measured OH reactivity value. These measurements can be compared to the calculated total reactivity from measured OH sinks (Eq. 2) to determine whether the measured total OH reactivity can be accounted for by the measured sinks. The difference between the measured and calculated total OH reactivity is referred to as the "missing" OH reactivity.

Laboratory measurements of the reactivity of several VOCs with well-known rate constants, including butane, isoprene, and propane showed that the OH reactivity measurements for these compounds were on average 30% lower than calculated when the measured velocity of the turbulent core is used to determine the reaction time. This consistent underestimation of the OH reactivity is likely due to either incomplete mixing of the reactants or a systematic underestimation of the reaction time (Hansen et al, 2014). As a result, the measured ambient OH reactivity values were scaled by a factor of 1.41. Measurements performed over a range of OH reactivity values suggest that the IU-TOHLM instrument can measure OH reactivity up to 45 s$^{-1}$ with a precision ($1\sigma$) of 1.2 s$^{-1}$ + 4% of the measured value for a 10 min average (Hansen et al., 2014).

**2.4 Modeling $HO_x$ concentrations and OH reactivity**

Ambient measurements of OH, $HO_2$\*, and total OH reactivity were modeled with the Regional Atmospheric Chemistry Mechanism (RACM2) (Goliff et al., 2013) and the Master Chemical Mechanism version 3.2 (Jenkin et al., 1997; Saunders et al., 2003). While the MCM model provides a near-explicit chemical mechanism and is expected to better represent complex chemical atmospheres, the lumped RACM mechanism is easier to use in radical budget calculations. The isoprene oxidation mechanism in RACM2 was updated as described in Tan et al. (2017) to include the Leuven Isoprene Mechanism (LIM1) originally proposed by Peeters, et al. (2009) involving peroxy radical isomerization reactions leading to additional $HO_x$ radical production, and includes the LIM1 updated bulk $RO_2$ reactions described in Peeters et al. (2014). The addition also includes a revision of the chemistry of first-generation isoprene oxidation products, including methyl vinyl ketone (MVK), methacrolein (MACR), and isoprene hydroperoxides (ISHP) (Tan et al., 2017). In addition, the ambient measurements were also modeled with version 3.3.1 of the Master Chemical Mechanism (MCM). In comparison to MCM 3.2, MCM 3.3.1 includes an updated isoprene oxidation mechanism based on the LIM1 mechanism resulting in $HO_x$ recycling from peroxy radical H-shift isomerization reactions (Jenkin et al., 2015).

The Framework for 0-D Atmospheric Modeling (F0AM) was used to calculate the radical concentrations and OH reactivity observed at the IRRONIC site (Wolfe et al., 2016). The model was constrained by the 30 minute average measured mixing ratios of ozone, $NO_x$, and VOCs and processed through a 5 day spin-up to generate unmeasured secondary oxidation products. Table S1 summarizes the measured compounds and includes their grouping into the condensed RACM2 model inputs. Because the VOC measurements occurred every 90 minutes, the measurements were interpolated into 30 min bins before input to the model. Due to the minimal overlap of the NO measurements with the $HO_x$ measurements, the model was constrained to the measured diurnal averaged mixing ratio of NO for all days. Zero-dimensional models cannot explicitly account for emissions, and NO is emitted both by vehicles on the nearby highway 1 km to the Southwest and by soil. Such local perturbations to the $NO_x$-$O_3$-radical chemistry necessitate using constrained measurements of NO, $NO_2$, and $O_3$. The measured $J(NO_2)$ was used to scale the model calculated $J(NO_2)$ and other photolysis rates. The model uncertainty is approximately 30% ($1\sigma$), estimated from uncertainties associated with the input parameters and the rate constants for each reaction (Griffith et al., 2013; Wolfe et al., 2016).

**3 Results and discussion**

Campaign diurnal average measurements of $J(NO_2)$, temperature, isoprene, $O_3$, $NO_2$, and NO are summarized in Fig. 1. The maximum average mixing ratio of NO of approximately 315 ppt was observed at approximately 08:00 (EDT), while the average mixing ratio of $NO_2$ reached a maximum of 2 ppb around 10:00. Average mixing ratios of isoprene ranged from 0.4 to 4.4 ppb, reaching a maximum around 18:00. Anthropogenic VOCs were relatively low at this site, with maximum mixing ratios of benzene less than 80 ppt. Day-to-day profiles (July 10 to July 25) are illustrated in Fig. 2, showing measurements of

9

1  $O_3$, temperature, isoprene, $NO_x$, $HO_2$*, and OH. Unfortunately, instrumental problems limited the NO measurements prior to

2  19 July.

**3.1 OH measurements and model comparison**

4  OH concentrations were determined using the chemical modulation technique described above using external $C_3F_6$ addition to

5  scavenge ambient OH and measure interferences producing OH inside the IU-FAGE detection cell, including laser generated

6  OH. The measured interferences were subtracted from the total OH signal determined from spectral modulation, resulting in

7  net ambient OH concentrations (Fig. 2). As can be seen from this figure, the measured interference was a significant fraction

8  of the total OH signal on many days.

9  Figure 3 illustrates the total measured OH radical signal by spectral modulation (black circles), the measured

10  interference (blue squares), and the expected laser-generated interference from reactions 3 and 4 calculated from laboratory

11  calibrations (Griffith et al., 2016) (green points) during 14 July and 15 July. On 15 July, the measured interference was similar

12  to the calculated interference suggesting that the majority of the measured interference was laser-generated. However, on 14

13  July, the measured interference was much larger than the calculated interference, suggesting that the majority of the measured

14  interference was due to an unknown source. Subtraction of the calculated laser-generated interference from the measured

15  interference on all days resulted in a measurement of the unknown interference that increased with both ozone and temperature

16  during the campaign (Fig. 4).

17  This result is consistent with the observations from Mao et al. (2012) who found that the interference measured in

18  their LIF-FAGE instrument using a similar chemical modulation technique increased with ozone and total OH reactivity. The

19  observed increase in the magnitude of the unknown interference with ozone and temperature suggests that the interference

20  may be related to the ozonolysis of biogenic VOCs, whose emissions increase with temperature. This result is also consistent

21  with the measurements of Novelli et al. (2017), who found that their observed interference correlated with the product of ozone

22  and biogenic VOC concentrations, although the correlation in the present study was not statistically significant. Previous

23  measurements have shown that some LIF-FAGE instruments, including the IU-FAGE instrument, are susceptible to an

24  interference under high concentrations of ozone and biogenic VOCs, perhaps due to the decomposition of Criegee

25  intermediates inside the FAGE detection cell (Novelli et al., 2014; Fuchs et al., 2016; Novelli et al., 2017; Rickly and Stevens,

26  2018). However, estimated concentrations of Criegee intermediates in similar environments on the order of $5\times10^4$ cm$^{-3}$ (Novelli

27  et al., 2017) are too low to explain the observed interference during the IRRONIC campaign.

28  The observation of a significant interference during this campaign is in contrast to previous measurements of OH by

29  the IU-FAGE instrument in a forested environment during the CABINEX 2009 campaign (Griffith et al., 2013). During this

30  campaign, several tests were conducted where $C_3F_6$ or CO was added to remove ambient OH. These tests did not reveal any

31  significant interference, and measurements of OH were found to be in good agreement with model predictions (Griffith et al.,

32  2013). One possible explanation for this discrepancy with the measurements during IRRONIC is the lower levels of ozone and

33  temperatures observed during CABINEX compared to IRRONIC. Average mixing ratios of ozone during CABINEX were

near 30 ppb and average temperatures were near 20°C during the day, with average mixing ratios of isoprene less than 2 ppb in the afternoon. These levels of ozone and temperature are lower than that where the interference was observed during IRRONIC (Fig. 4), suggesting that a similar interference was likely undetectable during CABINEX.

Recent measurements have found that $NO_3$ radicals can lead to an interference in FAGE instruments (Fuchs et al., 2016), although the mechanism for production of this interference is not known. Such an interference in the IU-FAGE instrument could explain the observed interference during some nights (Fig. 3), but is unlikely the source of the interference during the daytime. Another possible source of the interference is the decomposition of ROOOH molecules inside the FAGE detection cell formed from the reaction of OH with $RO_2$ radicals (Fittschen et al., 2019). However, assuming a rate constant of $1 \times 10^{-10}$ $cm^{-3}$ $s^{-1}$ for the OH + $RO_2$ reaction, it is unlikely that a significant fraction of $RO_2$ radicals will react to form ROOOH under the mixing ratios of NO observed at this site, as the estimated lifetime of $RO_2$ radicals with respect to reaction with NO was an order-of-magnitude shorter than that for reaction with OH. Additional measurements and laboratory tests will be needed to identify and minimize interferences associated with LIF-FAGE measurements of OH.

The day-to-day measurements of OH after the interference has been subtracted for 10-20 July and 24-25 July are illustrated in Fig. 5. Measurements on 21-22 July focused on measurements of $HO_2$* as part of the peroxy radical informal instrumental intercomparison (Kundu et al., 2019), with NO added continuously to the detection cell to provide measurements with a higher time resolution. Thus OH measurements were not conducted on these days. This figure also illustrates the day-to-day model results for OH and $HO_2$* from the MCM models 3.2 and 3.3.1 and the base RACM2 and the modified RACM2-LIM1 models, illustrating that, the predicted OH concentrations are generally lower than the measured concentrations.

Figure 6 (top) shows the average diurnal profile of the 15-min OH measurements, both with and without the measured interference, binned into 1 hour time periods for the days illustrated in Fig. 5. The average ambient diurnal OH radical concentration reached a maximum of approximately 4-5 $\times$ $10^6$ $cm^{-3}$ after the measured interference was subtracted. If the measured interference was not subtracted from the total OH signal determined by spectral modulation, the resulting OH radical concentrations would be as high as $9 \times 10^6$ $cm^{-3}$ (Fig. 6), much greater than the MCM and RACM2 modeled diurnal average maximum concentrations of approximately $2 \times 10^6$ $cm^{-3}$. The daytime OH radical concentration measurements after the interference has been subtracted are in better agreement with the model results, but are still approximately a factor of two larger from 12:00 to midnight and appear to peak later than the model predictions. Including versions of the LIM1 mechanism for $HO_x$ regeneration in both the MCM (3.3.1) and RACM2 (RACM2-LIM1) models result in somewhat higher modeled daytime concentrations of OH compared to the base MCM 3.2 and RACM2 mechanisms, although the results are still lower than the measured concentrations (Fig. 6).

A possible reason for the model underprediction of the measurements is an underestimation of the concentration of NO in the model. As discussed above, instrumental problems limited the measurements of NO primarily to several days at the end of the campaign, resulting in approximately 2-3 days that overlapped with the OH measurements (Fig. 2). Consistent measurements were only obtained after replacing the instrument's detector. In order to model the remaining days of the campaign, the model was constrained to the diurnal average of the NO measurements from the latter half of the campaign.

11

However, it is possible that the actual mixing ratio of NO during the early days of the campaign was higher than the average value measured during the end of the campaign, given that the measured $NO_2$ concentrations during the early part of the campaign were approximately a factor of 2 greater than that measured during the latter part of the campaign (20-24 July) (Fig. 2). For the days at the end of the campaign where there was significant overlap between the measurements of OH and NO, the model results are in better agreement during these days (20 and 24 July) (Fig. 5). On 20 July, the RACM2-LIM1 and MCM 3.3.1 models predict maximum OH concentrations that are within 30% of the measured OH on 20 July (Fig. S1).

The diurnal average model results are in better agreement with the measurements when mixing ratios of NO were unconstrained while constraining mixing ratios of $NO_2$ and $O_3$. As shown in Fig. 6, unconstraining the concentration of NO in the MCM models increases the predicted OH concentrations by approximately a factor of 3 during the daytime with model predicted mixing ratios of NO approximately a factor of 2 greater than the constrained values during the day. Similar results were found when NO was unconstrained in the RACM2 models (Fig. S2). However, the assumption that NO is in steady-state may not be justified given the location of the site near NO sources from transportation as well as the potential influence of soil emissions (Molina-Herrera et al., 2017). In addition, the measurements suggest that deviations from the ozone photostationary state were significant at this site, implying that the concentrations of peroxy radicals were high enough to significantly impact the concentration of NO. On the days when NO was measured, the models overpredicted the NO measurements by a factor of approximately 2-4 during the day, and underpredicted the measurements in the morning and evening (Fig. S3). This underprediction of the measured NO in the morning and evening may reflect active NO sources from soil and transportation emissions, and could explain why the NO unconstrained model underpredicts the concentration of OH in the afternoon. Although the model still underestimates the measurements of OH, it is clear that without taking the observed OH interference into account, the measured OH concentrations would have been a factor of 5 greater than predicted by the model mechanisms, similar to previous measurements under comparable mixing ratios of isoprene and $NO_x$ (Rohrer et al., 2014).

**3.2 $HO_2$* measurements and model comparison**

The day-to-day measurements of $HO_2$* are illustrated in Fig. 5 with the MCM 3.2, MCM 3.3.1, RACM2, and RACM2-LIM1, model results. The contribution of modeled $RO_2$ radicals to the modeled $HO_2$* is based on laboratory calibrations of the $RO_2$– to–$HO_2$ conversion efficiencies for the sampling conditions used in this study (Lew et al., 2018) and are incorporated into both versions of the RACM2, and MCM peroxy radical categories. Under the instrumental conditions during the campaign, the conversion efficiency of isoprene-based peroxy radicals to $HO_2$ was determined to be approximately 83 ± 7%, while the conversion efficiency of methyl peroxy radicals was estimated to be approximately 5% (Lew et al., 2018). These two peroxy radicals accounted for the majority of $RO_2$ radicals predicted by the models (see below). The maximum measured $HO_2$* concentration each day during the campaign was generally between approximately $2 \times 10^8$ and $2 \times 10^9$ molecules $cm^{-3}$ (Figs. 2 and 5), with an average daily maximum value of approximately $1 \times 10^9$ $cm^{-3}$ (Fig. 6). The RACM2-LIM1 and MCM 3.3.1 modeled diurnal averaged $HO_2$* reached a maximum of approximately $1.4 \times 10^9$ $cm^{-3}$ and $1.3 \times 10^9$ $cm^{-3}$, respectively, compared to a value of $1.2 \times 10^9$ $cm^{-3}$ for the RACM2 and MCM 3.2 modeled $HO_2$* (Fig. 6).

12

The predicted $HO_2$*concentrations by the base RACM2 model are in good agreement with the measured concentrations, overpredicting the measurements by approximately 20% on average, although the model agrees with the measurements to within the combined uncertainty of the model and the measurements. Including the LIM1 mechanism in the RACM2 mechanism increases the modeled $HO_2$* by approximately 15% due to the modeled increase in $HO_x$ radical production from the isomerization of isoprene-based peroxy radicals. These results are in contrast to that observed during the CABINEX campaign, where a RACM-based model overpredicted the measured $HO_2$* by as much as a factor of 2 (Griffith et al., 2013), likely related to the higher concentrations of NO observed during IRRONIC compared to CABINEX increasing the importance of the $HO_2$ + NO and $RO_2$ + NO reactions in determining the fate of these radicals.

The MCM-based model results are also in good agreement with the measured $HO_2$*, also overpredicting the measured concentrations by approximately 20% on average in the afternoon (Fig. 5 and 6). The MCM 3.3.1 mechanism results in predicted $HO_2$* concentrations that are approximately 5% greater than that predicted by MCM 3.2 in the afternoon when NO concentrations are low due to the inclusion of $HO_x$ production from the isomerization of isoprene-based peroxy radicals. These results are also consistent with a possible underestimation of the actual concentrations of NO at the site as discussed above. Unconstraining the mixing ratio of NO in the MCM models increase the averaged modeled $HO_2$* concentrations by approximately 10%, but they are still within the combined uncertainty of the model and the measurements (Fig. 6). Similar results were found when NO was unconstrained in the RACM2 models, although the higher daytime NO predicted by these models resulted in lower daytime $HO_2$* concentrations when compared to the NO constrained models, while the lower predicted nighttime NO resulted in predicted $HO_2$* concentrations by the base RACM2 model that were significantly greater compared to both the NO constrained model results and the measurements (Fig. S2).

The MCM 3.2 and MCM 3.3.1 diurnal average modeled $HO_2$* concentrations and the model contribution of peroxy radicals to $HO_2$* are shown in Fig. 7 (left panels). The diurnal profile of the $HO_2$* radical concentration predicted by the MCM models includes contributions primarily from isoprene peroxy radicals and $HO_2$ radicals, with smaller contributions from methyl peroxy and acetyl peroxy radicals (Fig. 7). The RACM2 models produced similar results, with $HO_2$ and isoprene peroxy radicals contributing to the majority of the modeled $HO_2$* concentrations (Fig. S4). The total modeled $RO_x$ ($RO_2$ + $HO_2$) concentrations by the different mechanisms are also shown in Fig. 7 (right panels). The MCM 3.2 model predicted that the diurnal average total $RO_x$ concentration consisted primarily of $HO_2$ (52%), isoprene peroxy radicals (20%), methyl peroxy ($CH_3O_2$, 22%), and acetyl peroxy ($CH_3CO_3$, 5%), with daytime (08:00 – 20:00) contributions of 48%, 26%, 19%, and 5% for $HO_2$, isoprene peroxy, $CH_3O_2$, and $CH_3CO_3$, respectively. The MCM 3.3.1 model predicted that $HO_2$ (53%), isoprene peroxy (16%), methyl peroxy (23%), acetyl peroxy (5%) were the major contributors to the modeled diurnal average total $RO_x$ concentration, with daytime contributions of 50%, 22%, 21%, and 6% (Fig. 7). Similar results were obtained from the RACM2 models (Fig. S4). As discussed above, the configuration of the IU-FAGE instrument used in this study converted approximately 83% of isoprene peroxy radicals to $HO_2$ upon addition of NO and minimally converts methyl peroxy radicals to $HO_2$ (<5%) (Lew et al., 2018). Thus, the majority of the contributing species to the measured $HO_2$* are $HO_2$ and isoprene peroxy radicals which together account for approximately 70% of the total peroxy radical concentration predicted by these models.

13

1 Measurements of the total $HO_2 + RO_2$ radical concentrations using an Ethane – Nitric Oxide Chemical Amplifier (ECHAMP)

2 were found to be in good agreement with the $HO_2*$ measurements reported here and are summarized in Kundu et al. (2019).

**3.3 Total OH reactivity measurements and model comparison**

4      The measured total OH reactivity and that calculated from measured OH sinks using both the RACM and MCM

5 mechanisms are shown in Fig. 8, where the measured OH reactivity is averaged into 2 hour bins. As illustrated in this figure,

6 the calculated OH reactivity was in relatively good agreement with the measured OH reactivity on some days and nights,

7 specifically 15-16 July, with missing reactivity observed later in the campaign. Overall, the averaged measured OH reactivity

8 varied between the instrumental limit of detection of 1 $s^{-1}$ to a maximum of approximately $31 s^{-1}$ with an overall diurnal average

9 value of approximately 13 $s^{-1}$.

10      The campaign diurnal averaged measured OH reactivity is shown in Fig. 9 along with the calculated total OH

11 reactivity from the measured OH sinks. On average, the calculated reactivity is in good agreement with the measurements. As

12 expected for this deciduous forest environment, isoprene was the dominant contributor making up 37% of the diurnally

13 averaged total reactivity, followed by OVOCs (28%), inorganics (10%), alkanes and alkenes (5%), anthropogenic non-methane

14 hydrocarbons (NMHC) (1%), and monoterpenes (<1%) with missing reactivity accounting for the remaining 18% (Fig. S5).

15 During the daytime (08:00 and 20:00) the contributions are similar, with isoprene being the largest contributor at 47% followed

16 by OVOCs (24%), inorganics (8%), alkanes and alkenes (4%), anthropogenic NMHC (1%), and monoterpenes (<1%) with

17 missing reactivity accounting for the remaining 14%. During the nighttime, (20:00 to 08:00), OVOCs were the dominant

18 contributor to the modeled OH reactivity at 32% followed by isoprene (24%), inorganics (11%), alkanes and alkenes (6%),

19 anthropogenic NMHC (2%), and monoterpenes (<1%) with missing reactivity of 24% (Fig. S5).

20      The campaign diurnal average (Fig. 9) shows a correlation with temperature, with the maximum average OH

21 reactivity of approximately 20 $s^{-1}$ occurring around 13:30. The calculated reactivity was consistent with the measured reactivity

22 for temperatures less than 294 K, while the observed reactivity is greater than that calculated from the measured sinks for

23 higher temperatures, although at temperatures above 302 K the measured reactivity appears to be less than calculated (Fig.

24 S6). These results are similar to that reported by Hansen et al. (2014) and Di Carlo et al. (2004) in which the measured missing

25 reactivity appeared to increase with temperature.

26      Figure 9 also shows the campaign average OH reactivity including the reactivity of unmeasured oxidation products

27 predicted by the MCM 3.3.1 model. On average, including the contribution of unmeasured oxidation products can account for

28 the majority of the missing reactivity. While the model tends to overpredict the average measured reactivity in the afternoon

29 and evening, the model results agree to within the combined uncertainty of the model and the precision of the measurement

30 (Hansen et al., 2014). Similar results were obtained by the RACM2 models, although the predicted reactivity of unmeasured

31 oxidation products by the RACM2 models are approximately a factor of two smaller than that predicted by the MCM models

32 (Fig. S7). These results suggest that the models are generally able to reproduce the measured OH reactivity at this site, and

1    that the missing reactivity observed during IRRONIC may be due to unmeasured oxidation products, with isoprene nitrates

2    and isoprene epoxides within the RACM2 and MCM mechanisms being the primary contributors to the missing reactivity.

3         While the campaign averaged OH reactivity measurements appear to be in reasonable agreement with the calculated

4    reactivity based on measured compounds, there were several days that displayed large missing reactivity similar to that

5    observed by Hansen et al. (2014). The MCM 3.3.1 model results for a day with the largest missing reactivity (17 July) is shown

6    in Fig. 10, indicating that the modeled reactivity including unmeasured oxidation products cannot explain the observed

7    reactivity on this day. The reason for this discrepancy is unclear, as the missing reactivity on this day did not appear to correlate

8    with changes in wind speed, direction, trajectory, or meteorological conditions, but may indicate the presence of additional

9    unmeasured emissions or oxidation products not accounted for by the model. Additional measurements and analyses will be

10   necessary to determine the source of the missing reactivity.

11   **3.4 Radical budgets**

12        The analysis of the rates of radical initiation, propagation, and termination can provide insight to the importance of

13   individual radical sources and sinks. For the IRRONIC campaign, the OH radical budget is illustrated in Fig. 11, where OH

14   radical production reactions are represented in shades of blue and loss reactions are represented in shades of red. Daytime

15   production includes reactions with both initiation and propagation that produces OH radicals (positive rates), while daytime

16   OH loss reactions are represented by propagation and termination reactions that remove OH (negative rates). For simplicity

17   only the RACM2 and RACM2-LIM1 radical budgets are shown.

18        The maximum rates for the OH radical budget of approximately $2.7 \times 10^7$ cm$^{-3}$ s$^{-1}$ from the RACM2-LIM1 model

19   were higher than the maximum value of $2.2 \times 10^7$ cm$^{-3}$ s$^{-1}$ in RACM2. The addition of the LIM1 mechanism increases the OH

20   radical production rate mostly from photolysis of hydroxyperoxy aldehydes (HPALD) produced from the isomerization of

21   isoprene-based peroxy radicals and their subsequent chemistry (Peeters et al., 2014; Tan et al., 2017). In the RACM2-LIM1

22   model, the daytime OH radical production is dominated by the $HO_2$ + NO reaction from 10:00 to 14:00 (59%) and drops to

23   29% from 14:00 to 18:00. Ozone photolysis and the LIM1 mechanism contribute up to 31% and 20% of the total OH radical

24   production from 14:00 to 18:00, with ozonolysis (VOC+$O_3$) and photolysis of HONO, $H_2O_2$, methacrolein (MACR), and

25   organic peroxides (OP1, OP2) contributing to 8% and 10% of the total OH radical production in the afternoon (Fig. 11). A

26   majority of the OH radical loss is due to OH reactions with VOCs (63-68%) and OVOCs (29-26%) during the morning and

27   afternoon. As described above, the measured total OH reactivity was in reasonable agreement with the modeled OH reactivity;

28   therefore, it is likely that the total OH loss is well represented in the model. An experimental radical budget for 20 July when

29   the measurements were complete suggests that the total measured OH production rate is nearly balanced by the total OH loss

30   rate calculated by the concentration of individual sinks and the loss rate based on the measured total OH reactivity to within

31   approximately 30% (Fig. S8), consistent with the agreement between the measured and modeled OH on this day as discussed

32   above. For simplicity, the measured $HO_2$* was used to calculate the rate of OH production from the $HO_2$ + NO reaction and

33   as a result the measured production rate represents an upper limit to the overall OH production rate. Thus, the difference

The total radical ($RO_x$) budget from the RACM2 mechanisms of OH, $HO_2$, and $RO_2$ radicals is illustrated in Fig. 12. Overall, total radical initiation in the RACM2-LIM1 mechanism was larger, with a maximum value of approximately $3.2 \times 10^7$ cm$^{-3}$ s$^{-1}$ compared to RACM2 maximum value of approximately $2.2 \times 10^7$ cm$^{-3}$ s$^{-1}$. The increase in total radical initiation in the RACM2-LIM1 model is due to both the added radical initiation from the photolysis of HPALDs as well as increased radical initiation from other aldehydes produced in the LIM1 mechanism. Overall, radical initiation from the photolysis of HPALDs and the subsequent chemistry from the LIM1 mechanism contributed 16-22% of total radical initiation during the day, while photolysis of formaldehyde and other aldehydes contributed to approximately 42% of total radical initiation, with ozone photolysis contributing to 29-33% of radical initiation in the mornings and afternoon (Fig. 12). In contrast, ozone photolysis contributes to approximately 43% of radical initiation in the RACM2 mechanism compared to formaldehyde and other aldehydes contributing 22-24% (Fig. 12). Radical termination for both mechanisms is dominated by peroxy radical self-reactions, such as the $HO_2 + HO_2$ reaction, as well as the reaction of $HO_2$ with isoprene-based peroxy radicals (ISOP) and other peroxy radicals ($RO_2$). These reactions account for approximately 80% of radical termination due to the low levels of $NO_x$ used in the models, with reaction of OH +$NO_2$ and other $NO_x$ radical reactions accounting for approximately 20% of radical termination in these models (Fig. 12). As discussed above, it is possible that the NO concentration used to constrain the model may be lower than the actual concentration. As a result, the modeled contribution of $NO_x$ reactions to radical termination may represent a lower limit to the actual contribution.

The partitioning of the total radical budget production for IRRONIC is similar to the modeled budget observed during PROPHET 2008 and CABINEX 2009 (Griffith et al., 2013). The updated RACM model used during these campaigns predicted that radical termination was dominated by $HO_2 + RO_2$ reactions (including the HO2 + ISOP reaction), contributing to approximately 80% of total radical termination, similar to the 74% for the $HO_2$+ISOP and $HO_2$+$RO_2$ reactions predicted here by the RACM2 model. The photolysis of ozone accounted for approximately 20-30% of total radical initiation during these campaigns based on an updated version of the RACM model (Griffith et al., 2013) compared to approximately 40% predicted by the RACM2 mechanism during IRRONIC due to higher concentrations observed during this campaign. Ozonolysis reactions contributed to approximately 20-30% of total radical initiation during PROPHET and CABINEX compared to 10-11% during IRRONIC. Photolysis of HCHO and other aldehydes contributed to approximately 22-24% of the total rate of radical initiation during IRRONIC compared to 23% and 5% during PROPHET 2008 and CABINEX 2009, respectively, with the low contribution during CABINEX primarily due to the lower mixing ratios of HCHO observed during this campaign (Griffith et al., 2013). In contrast, photolysis of HONO was a significant radical source during PROPHET and CABINEX, contributing 14-17% of radical initiation compared to approximately 3% of total radical production during IRRONIC due to the lower mixing ratios of HONO observed during IRRONIC. On average, mixing ratios of HONO during IRRONIC were approximately 40 ppt at night decreasing to approximately 10 ppt during the day (Fig. S9) compared to daytime mixing ratios

16

between 50 and 75 ppt during PROPHET and CABINEX (Griffith et al., 2013). The reason for the difference in the measured HONO values between these two sites is unclear, but may be related to increased production from photolysis of nitric acid on the forest canopy surfaces at the PROPHET site (Zhou et al., 2011).

**4 Summary**

Measurements of OH radical concentrations using the IU-FAGE instrument during the IRRONIC campaign revealed a significant unknown interference that appeared to correlate with both temperature and ozone. The average measured OH radical concentration after the interference was subtracted reached an average daytime maximum of approximately $4\text{-}5 \times 10^6$ $cm^{-3}$. This is in contrast to the measurements including the interference which reached an average daytime maximum of approximately $9 \times 10^6$ $cm^{-3}$. Similar concentrations of OH were observed at this site in 2017 during an informal intercomparison between the IU-FAGE instrument and the University of Colorado Chemical Ionization Mass Spectrometry (CIMS) instrument (Rosales et al., 2018; Reidy et al., 2018).

After subtracting the interference, the OH measurements were in better agreement with model simulations utilizing the Regional Atmospheric Chemical Mechanism 2 (RACM2) with an updated Leuven Isoprene Mechanism (LIM1) as well as the Master Chemical Mechanism versions 3.2 and 3.3.1. Both the RACM2-LIM1 and MCM 3.3.1 mechanisms add radical recycling reactions for isoprene oxidation that increase the modeled OH and peroxy radical concentrations. The addition of radical recycling by isoprene still resulted in model predictions of OH that were approximately a factor of two lower than the measured concentrations. One possible explanation for the discrepancy is an underestimation of the mixing ratio of NO during the campaign, as instrumental difficulties prevented measurements of NO except at the end of the campaign. Unconstraining the mixing ratio of NO in the model while constraining $NO_2$ and $O_3$ to their measured values leads to an increase in the modeled mixing ratios of NO resulting in an increase in the average modeled OH concentration by approximately a factor of 2-3, improving the agreement with the measured OH concentrations. These higher values of $NO_x$ are comparable to that observed at this site in 2017 when measured OH concentrations were similar to that observed here (Rosales et al., 2018; Reidy et al., 2018). However, it is clear that if the measured interference was not taken into account, the apparent OH concentrations would have been a factor of 5 greater than predicted by the model mechanisms, comparable to previous measurements under low $NO_x$ and high isoprene conditions (Rhorer et al., 2014). These results are similar to that reported by Mao et al. (2012) and Mallik et al. (2017) who found good agreement between their OH measurements and model predictions when measured interferences were taken into account. However, because of differences in instrument design (geometry, cell pressure, flow, etc.) these interferences may not significantly impact other LIF-FAGE instruments. However, future OH measurements using the LIF-FAGE technique should include methods to quantify potential instrumental artifacts even if they are insignificant, to demonstrate that the measurements are free from interferences.

Measurements of total OH reactivity were in reasonable agreement with that calculated from measured OH sinks, with isoprene contributing approximately 37% and OVOCs 28% of the diurnally averaged measured reactivity, with 18% of

the measured reactivity missing. However, on average the missing reactivity fraction can be explained by unmeasured oxidation products, specifically from isoprene nitrates and isoprene epoxides within the RACM2 and MCM mechanisms. This indicates that these mechanisms are accurately representing the total OH loss at this site.

Measurements of $HO_2$ radicals by the IU-FAGE instrument using chemical conversion to OH by addition of NO has been shown to be sensitive to alkene-based peroxy radicals (Lew et al., 2018). As a result, the measurements represent a sum of $HO_2$ and a fraction of $RO_2$ radicals in the atmosphere ($HO_2$*). During the IRRONIC campaign, the measured $HO_2$* concentration primarily reflected the sum of $HO_2$ and isoprene-based peroxy radicals, which contributed to approximately 70% of the total modeled peroxy radicals. The average daytime ambient $HO_2$* measurements reached maximum concentrations of approximately $1 \times 10^9$ $cm^{-3}$. Both MCM models predicted $HO_2$* concentrations that were in good agreement with the measurements, while the RACM mechanisms resulting in predicted concentrations that were approximately 20-35% greater than the measurements but within the combined uncertainty of both the model and the measurement. These results are also consistent with an underestimation of the NO concentrations in the model, as increasing the modeled NO resulted in modeled $HO_2$* concentrations that were still in good agreement with the measurements. These results are in contrast to some previous measurements in forest environments where model predictions were found to be significantly greater than measured $HO_2$* concentrations (Griffith et al., 2013), perhaps as a result of the lower mixing ratios of NO observed at these sites. Additional measurements are needed in order to resolve this discrepancy, which may be related to a gap in our understanding of peroxy radical chemistry under low NO conditions.

**Data availability.** Data are available upon request from the corresponding author (pstevens@indiana.edu).

**Competing interests.** The authors declare that they have no conflicts of interest.

**Author contributions.** PS, SD and EW designed the research project. ML, PR, BB, and PS were responsible for the LIF-FAGE OH, $HO_2$*, OH reactivity, and HONO measurements. SK and EW were responsible for the supporting measurements of NO, $NO_2$, and $O_3$. SD, SS, TL, and NL were responsible for the measurements of VOCs and OVOCs. ML, PR, ER, and PS conducted the analysis and photochemical modelling and wrote the paper with feedback from all co-authors. ML and PR contributed equally to the paper.

## References

Ait-Helal, W., Borbon, A., Sauvage, S., de Gouw, J. A., Colomb, A., Gros, V., Freutel, F., Crippa, M., Afif, C., Baltensperger, U., Beekmann, M., Doussin, J.-F., Durand-Jolibois, R., Fronval, I., Grand, N., Leonardis, T., Lopez, M., Michoud, V., Miet, K., Perrier, S., Prévôt, A. S. H., Schneider, J., Siour, G., Zapf, P., and Locoge, N.: Volatile and intermediate volatility organic compounds in suburban Paris: variability, origin and importance for SOA formation, Atmos. Chem. Phys., 14, 10439–10464, 2014

Badol, C., Borbon, A., Locoge, N., Leonardis, T., and Galloo, J. C.: An automated monitoring system for VOC ozone precursors in ambient air: development, implementation and data analysis, Anal. Bioanal. Chem., 378, 7, 1815–1827, 2004.

Bottorff, B., Stevens, P. S., Lew, M., Rickly, P., and Dusanter, S. Measurements of Nitrous Acid (HONO) in an Indiana Forest by Laser Photofragmentation/Laser-Induced Flourescence (LP/LIF), Abstract A21B-0116 presented at 2015 Fall Meeting, AGU, San Francisco, CA, 14-18 Dec., 2015.

Carslaw, N., Creasey, D. J., Harrison, D., Heard, D. E., Hunter, M. C., Jacobs, P. J., Jenkin, M. E., Lee, J. D., Lewis, A. C., Pilling, M. J., Saunders, S. M., and Seakins, P. W.: OH and $HO_2$ Radical Chemistry in a Forested Region of North-Western Greece, Atmos. Environ., 35, 4725-4737, 2001.

Chen, S., Ren, X., Mao, J., Chen, Z., Brune, W. H., Lefer, B., Rappenglück, B., Flynn, J., Olson, J., and Crawford, J. H.: A Comparison of Chemical Mechanisms Based on Tramp-2006 Field Data, Atmos. Environ., 44, 4116-4125, 2010.

Creasey, D. J., Heard, D. E., and Lee, J. D.: Eastern Atlantic Spring Experiment 1997 (Ease97) 1. Measurements of OH and $HO_2$ Concentrations at Mace Head, Ireland, J. Geophys. Res., 107, 10.1029/2001jd000892, 2002.

Crowley, J. N., Pouvesle, N., Phillips, G. J., Axinte, R., Fischer, H., Petäjä, T., Nölscher, A., Williams, J., Hens, K., Harder, H., Martinez-Harder, M., Novelli, A., Kubistin, D., Bohn, B., and Lelieveld, J.: Insights into $HO_x$ and $RO_x$ chemistry in the boreal forest via measurement of peroxyacetic acid, peroxyacetic nitric anhydride (PAN) and hydrogen peroxide, Atmos. Chem. Phys., 18, 13457–13479, 2018.

Czader, B. H., Li, X., and Rappenglueck, B.: Cmaq Modeling and Analysis of Radicals, Radical Precursors, and Chemical Transformations, J. Geophys. Res., 118, 11,376-311,387, 10.1002/jgrd.50807, 2013.

Davis, D. D., Rodgers, M. O., Fischer, S. D., and Asai, K.: An Experimental Assessment of the $O_3/H_2O$ Interference Problem in the Detection of Natural Levels of OH Via Laser Induced Fluorescence, Geophys. Res. Lett., 8, 69-72, 10.1029/GL008i001p00069, 1981a.

Davis, D. D., Rodgers, M. O., Fischer, S. D., and Heaps, W. S.: A Theoretical Assessment of the $O_3/H_2O$ Interference Problem in the Detection of Natural Levels of OH Via Laser Induced Fluorescence, Geophys. Res. Lett., 8, 73-76, 10.1029/GL008i001p00073, 1981b.

Detournay, A., Sauvage, S., Locoge, N., Gaudion, V., Leonardis, T., Fronval, I., Kaluzny, P., and Galloo, J.-C.: Development of a sampling method for the simultaneous monitoring of straightchain alkanes, straight-chain saturated carbonyl compounds and monoterpenes in remote areas, J. Environ. Monit., 13, 983–990, 2011.

Di Carlo, P., Brune, W. H., Martinez, M., Harder, H., Lesher, R., Ren, X., Thornberrry, T., Carroll, M. A., Young, V., Shepson, P. B., Riemer, D., Apel, E., and Campbell, C.: Missing OH Reactivity in a Forest: Evidence for Unknown Reactive Biogenic VOCs. Science, 304, 5671, 2004.

Dusanter, S., Vimal, D., and Stevens, P. S.: Technical Note: Measuring Tropospheric OH and $HO_2$ by Laser-Induced Fluorescence at Low Pressure. A Comparison of Calibration Techniques, Atmos. Chem. Phys., 8, 321-340, 2008.

Dusanter, S., Vimal, D., Stevens, P. S., Volkamer, R., and Molina, L. T.: Measurements of OH and $HO_2$ concentrations during the MCMA-2006 field campaign – Part 1: Deployment of the Indiana University laser-induced fluorescence instrument, Atmos. Chem. Phys., 9, 1665–1685, 2009a.

Dusanter, S., Vimal, D., Stevens, P. S., Volkamer, R., Molina, L. T., Baker, A., Meinardi, S., Blake, D., Sheehy, P., Merten, A., Zhang, R., Zheng, J., Fortner, E. C., Junkermann, W., Dubey, M., Rahn, T., Eichinger, B., Lewandowski, P., Prueger, J., and Holder, H.: Measurements of OH and $HO_2$ Concentrations During the MCMA-2006 Field Campaign – Part 2: Model Comparison and Radical Budget, Atmos. Chem. Phys., 9, 6655-6675, 2009b.

Dusanter S. and Stevens, P. S.: Recent Advances in the Chemistry of OH and $HO_2$ Radicals in the Atmosphere: Field and Laboratory Measurements, in Advances in Atmospheric Chemistry, Volume 1, John R. Barker, Allison L. Steiner, and Timothy J. Wallington, Editors, World Scientific Publishing Co. Pte. Ltd, New Jersey, pp. 493-579, 2017.

Emmerson, K. M., Carslaw, N., Carpenter, L. J., Heard, D. E., Lee, J. D., and Pilling, M. J.: Urban Atmospheric Chemistry During the Puma Campaign 1: Comparison of Modelled OH and $HO_2$ Concentrations with Measurements, J. Atmos. Chem., 52, 143-164, 2005.

Emmerson, K. M., Carslaw, N., Carslaw, D. C., Lee, J. D., McFiggans, G., Bloss, W. J., Gravestock, T., Heard, D. E., Hopkins, J., Ingham, T., Pilling, M. J., Smith, S. C., Jacob, M., and Monks, P. S.: Free Radical Modelling Studies During the UK Torch Campaign in Summer 2003, Atmos. Chem. Phys., 7, 167-181, 2007.

Fittschen, C., Al Ajami, M., Batut, S., Ferracci, V., Archer-Nicholls, S., Archibald, A. T., and Schoemaecker, C.: ROOOH: a missing piece of the puzzle for OH measurements in low-NO environments? Atmos. Chem. Phys., 19, 349-362, 2019.

Fuchs, H., Bohn, B., Hofzumahaus, A., Holland, F., Lu, K. D., Nehr, S., Rohrer, F., and Wahner, A.: Detection of HO2 by Laser-Induced Fluorescence: Calibration and Interferences from $RO_2$ Radicals, Atmos. Meas. Tech., 4, 1209-1225, 2011.

Fuchs, H., Tan, Z., Hofzumahaus, A., Broch, S., Dorn, H. P., Holland, F., Künstler, C., Gomm, S., Rohrer, F., Schrade, S., Tillmann, R., and Wahner, A.: Investigation of Potential Interferences in the Detection of Atmospheric $RO_x$ Radicals by Laser-Induced Fluorescence under Dark Conditions, Atmos. Meas. Tech., 9, 1431-1447, 2016.

George, L. A., Hard, T. M., and O'Brien, R. J.: Measurement of Free Radicals OH and $HO_2$ in Los Angeles Smog, J. Geophys. Res., 104, 11643-11655, 10.1029/1998jd100113, 1999.

Goliff, W. S., Stockwell, W. R., and Lawson, C. V.: The Regional Atmospheric Chemistry Mechanism, Version 2, Atmos. Environ., 68, 174-185, 2013.

Griffith, S. M., Hansen, R. F., Dusanter, S., Stevens, P. S., Alaghmand, M., Bertman, S. B., Car-roll, M. A., Erickson, M., Galloway, M., Grossberg, N., Hottle, J., Hou, J., Jobson, B. T., Kammrath, A., Keutsch, F. N., Lefer, B. L., Mielke, L. H., O'Brien, A., Shepson, P. B., Thurlow, M., Wallace, W., Zhang, N., and Zhou, X. L.: OH and $HO_2$ Radical Chemistry During PROPHET 2008 and CABINEX 2009 - Part 1: Measurements and Model Comparison, Atmos. Chem. Phys., 13, 5403-5423, 2013.

Griffith, S. M., Hansen, R. F., Dusanter, S., Michoud, V., Gilman, J. B., Kuster, W. C., Veres, P. R., Graus, M., de Gouw, J. A., Roberts, J., Young, C., Washenfelder, R., Brown, S. S., Thalman, R., Waxman, E., Volkamer, R., Tsai, C., Stutz, J., Flynn, J. H., Grossberg, N., Lefer, B., Alvarez, S. L., Rappenglueck, B., Mielke, L. H., Osthoff, H. D., and Stevens, P. S.: Measurements of Hydroxyl and Hydroperoxy Radicals During CalNex-LA: Model Comparisons and Radical Budgets, J. Geophys. Res., 121, 4211-4232, 10.1002/2015JD024358, 2016.

Hansen, R. F., Griffith, S. M., Dusanter, S., Rickly, P. S., Stevens, P. S., Bertman, S. B., Carroll, M. A., Erickson, M. H., Flynn, J. H., Grossberg, N., Jobson, B. T., Lefer, B. L., and Wallace, H. W.: Measurements of total hydroxyl radical reactivity during CABINEX 2009 – Part 1: field measurements. Atmos. Chem. Phys., 14, 2923-2937, 2014.

Heard, D. E., and Pilling, M. J.: Measurement of OH and $HO_2$ in the Troposphere, Chem. Rev., 103, 5163-5198, 2003.

Hens, K., Novelli, A., Martinez, M., Auld, J., Axinte, R., Bohn, B., Fischer, H., Keronen, P., Kubistin, D., Nölscher, A. C., Oswald, R., Paasonen, P., Petäjä, T., Regelin, E., Sander, R., Sinha, V., Sipilä, M., Taraborrelli, D., Tatum Ernest, C., Williams, J., Lelieveld, J., and Harder, H.: Observation and Modelling of $HO_x$ Radicals in a Boreal Forest, Atmos. Chem. Phys., 14, 8723-8747, 2014.

Hofzumahaus, A., Rohrer, F., Lu, K., Bohn, B., Brauers, T., Chang, C.-C., Fuchs, H., Holland, F., Kita, K., Kondo, Y., Li, X., Lou, S., Shao, M., Zeng, L., Wahner, A., and Zhang, Y.: Amplified Trace Gas Removal in the Troposphere, Science, 324, 1702-1704, 2009.

Holland, F., Hofzumahaus, A., Schäfer, J., Kraus, A., and Pätz, H.-W.: Measurements of OH and $HO_2$ Radical Concentrations and Photolysis Frequencies During Berlioz, J. Geophys. Res., 108, 8246, doi:8210.1029/2001JD001393, 2003.

Jenkin, M. E., Saunders, S. M., Pilling, M. J. The Tropospheric Degradation of Volatile Organic Compounds: A Protocol for Mechanism Development, Atmos. Environ., 31, 81, 1997.

Jenkin, M. E., Young, J. C., and Rickard, A. R.: The MCM v3.3.1 degradation scheme for isoprene, Atmos. Chem. Phys., 15, 11433-11459, 2015.

Kanaya, Y., Sadanaga, Y., Hirokawa, J., Kajii, Y., and Akimoto, H.: Development of a Ground-Based LIF Instrument for Measuring $HO_x$ Radicals: Instrumentation and Calibrations, J. Atmos. Chem., 38, 73-110, 2001.

Kanaya, Y., Cao, R., Akimoto, H., Fukuda, M., Komazaki, Y., Yokouchi, Y., Koike, M., Tanimoto, H., Takegawa, N., and Kondo, Y.: Urban Photochemistry in Central Tokyo: 1. Observed and Modeled OH and $HO_2$ Radical Concentrations During the Winter and Summer of 2004, J. Geophys. Res., 112, 10.1029/2007jd008670, 2007a.

Kanaya, Y., Cao, R., Kato, S., Miyakawa, Y., Kajii, Y., Tanimoto, H., Yokouchi, Y., Mochida, M., Kawamura, K., and Akimoto, H.: Chemistry of OH and $HO_2$ Radicals Observed at Rishiri Island, Japan, in September 2003: Missing Daytime Sink of $HO_2$ and Positive Nighttime Correlations with Monoterpenes, J. Geophys. Res., 112, doi:10.1029/2006JD007987, 2007b.

Kanaya, Y., Hofzumahaus, A., Dorn, H. P., Brauers, T., Fuchs, H., Holland, F., Rohrer, F., Bohn, B., Tillmann, R., Wegener, R., Wahner, A., Kajii, Y., Miyamoto, K., Nishida, S., Watanabe, K., Yoshino, A., Kubistin, D., Martinez, M., Rudolf, M., Harder, H., Berresheim, H., Elste, T., Plass-Dülmer, C., Stange, G., Kleffmann, J., Elshorbany, Y., and Schurath, U.: Comparisons of Observed and Modeled OH and $HO_2$ Concentrations During the Ambient Measurement Period of the HOxComp Field Campaign, Atmos. Chem. Phys., 12, 2567-2585, 2012.

Kim, S., Wolfe, G. M., Mauldin, L., Cantrell, C., Guenther, A., Karl, T., Turnipseed, A., Green-berg, J., Hall, S. R., Ullmann, K., Apel, E., Hornbrook, R., Kajii, Y., Nakashima, Y., Keutsch, F. N., DiGangi, J. P., Henry, S. B., Kaser, L., Schnitzhofer, R., Graus, M., Han-sel, A., Zheng, W., and Flocke, F. F.: Evaluation of $HO_x$ Sources and Cycling Using Measurement-Constrained Model Calculations in a 2-Methyl-3-Butene-2-ol (MBO) and Monoterpene (MT) Dominated Ecosystem, Atmos. Chem. Phys., 13, 2031-2044, 2013.

Konrad, S., Schmitz, T., Buers, H. J., Houben, N., Mannschreck, K., Mihelcic, D., Müsgen, P., Pätz, H. W., Holland, F., Hofzumahaus, A., Schäfer, H. J., Schröder, S., Volz-Thomas, A., Bächmann, K., Schlomski, S., Moortgat, G., and Großmann, D.: Hydrocarbon Measurements at Pabstthum During the Berlioz Campaign and Modeling of Free Radicals, J. Geophys. Res., 108, 8251, 10.1029/2001jd000866, 2003.

Kubistin, D., Harder, H., Martinez, M., Rudolf, M., Sander, R., Bozem, H., Eerdekens, G., Fischer, H., Gurk, C., Klüpfel, T., Königstedt, R., Parchatka, U., Schiller, C. L., Stickler, A., Taraborrelli, D., Williams, J., and Lelieveld, J.: Hydroxyl Radicals in the Tropical Troposphere over the Suriname Rainforest: Comparison of Measurements with the Box Model Mecca, Atmos. Chem. Phys., 10, 9705-9728, 2010.

Kundu, S., Deming, B. L., Lew, M. M., Bottorff, B. P., Rickly, P., Stevens, P. S., Dusanter, S., Sklaveniti, S., Leonardis, T., Locoge, N., and Wood, E. C.: Peroxy Radical Measurements by ethane – nitric oxide chemical amplification and laser-induced fluorescence during the IRRONIC field campaign in a forest in Indiana, Atmos. Chem. Phys. 19, 9563-9579, 2019.

Lelieveld, J., Butler, T. M., Crowley, J. N., Dillon, T. J., Fischer, H., Ganzeveld, L., Harder, H., Lawrence, M. G., Martinez, M., Taraborrelli, D., and Williams, J.: Atmospheric Oxidation Capacity Sustained by a Tropical Forest, Nature, 452, 737-740, 2008.

Levy, H.: Photochemistry of the Lower Troposphere, Planetary and Space Science, 20, 919-935, 1972.

Lew, M. M., Dusanter, S., and Stevens, P. S.: Measurement of Interferences Associated with the Detection of the Hydroperoxy Radical in the Atmosphere Using Laser-Induced Fluorescence, Atmos. Meas. Tech., 11, 95–109, 2018.

Lu, K. D., Hofzumahaus, A., Holland, F., Bohn, B., Brauers, T., Fuchs, H., Hu, M., Häseler, R., Kita, K., Kondo, Y., Li, X., Lou, S. R., Oebel, A., Shao, M., Zeng, L. M., Wahner, A., Zhu, T., Zhang, Y. H., and Rohrer, F.: Missing OH Source in a Suburban Environment near Beijing: Observed and Modelled OH and $HO_2$ Concentrations in Summer 2006, Atmos. Chem. Phys., 13, 2013.

Mallik, C., Tomsche, L., Bourtsoukidis, E., Crowley, J. N., Derstroff, B., Fischer, H., Hafermann, S., Hüser, I., Javed, U., Keßel, S., Lelieveld, J., Martinez, M., Meusel, H., Novelli, A., Phillips, G. J., Pozzer, A., Reiffs, A., Sander, R., Taraborrelli, D., Sauvage, C., Schuladen, J., Su, H., Williams, J., and Harder, H.: Oxidation processes in the eastern Mediterranean atmosphere: evidence from the modelling of $HO_x$ measurements over Cyprus, Atmos. Chem. Phys., 18, 10825–10847, 2018.

Mao, J., Ren, X., Zhang, L., Van Duin, D. M., Cohen, R. C., Park, J. H., Goldstein, A. H., Pau-lot, F., Beaver, M. R., Crounse, J. D., Wennberg, P. O., DiGangi, J. P., Henry, S. B., Keutsch, F. N., Park, C., Schade, G. W., Wolfe, G. M., Thornton, J. A., and Brune, W. H.: Insights into Hydroxyl Measurements and Atmospheric Oxidation in a California Forest, Atmos. Chem. Phys., 12, 8009-8020, 2012.

Martinez, M., Harder, H., Kovacs, T. A., Simpas, J. B., Bassis, J., Lesher, R., Brune, W. H., Frost, G. J., Williams, E. J., Stroud, C. A., Jobson, B. T., Roberts, J. M., Hall, S. R., Shetter, R. E., Wert, B., Fried, A., Alicke, B., Stutz, J., Young, V. L., White, A. B., and Zamora, R. J.: OH and $HO_2$ Concentrations, Sources, and Loss Rates During the Southern Oxidants Study in Nashville, Tennessee, Summer 1999, J. Geophys. Res., 108, 10.1029/2003jd003551, 2003.

Michoud, V., Kukui, A., Camredon, M., Colomb, A., Borbon, A., Miet, K., Aumont, B., Beekmann, M., Durand-Jolibois, R., Perrier, S., Zapf, P., Siour, G., Ait-Helal, W., Locoge, N., Sauvage, S., Afif, C., Gros, V., Furger, M., Ancellet, G., and Doussin, J. F.: Radical Budget Analysis in a Suburban European Site During the Megapoli Summer Field Campaign, Atmos. Chem. Phys., 12, 11951-11974, 2012.

Molina-Herrera, S., Haas, E., Grote, R., Kiese, R., Klatt, S., Kraus, D., Kampffmeyer, T., Friedrich, R., Andreae, H., Loubet, B., Ammann, C., Horváth, L., Larsen, K., Gruening, C., Frumau, A., Butterbach-Bahl, K. Importance of soil NO emissions for the total atmospheric $NO_x$ budget of Saxony, Germany, Atmos. Environ., 152, 61-76, 2017.

Nölscher, A. C., Yañez-Serrano, A. M., Wolff, S., de Araujo, A. C., Lavrič, J. V., Kesselmeier, J., and Williams, J.: Unexpected seasonality in quantity and composition of Amazon rainforest air reactivity, Nature Communications, https://doi.org/10.1038/ncomms10383, 2016.

Novelli, A., Hens, K., Tatum Ernest, C., Kubistin, D., Regelin, E., Elste, T., Plass-Dülmer, C., Martinez, M., Lelieveld, J., and Harder, H.: Characterisation of an inlet pre-injector laser-induced fluorescence instrument for the measurement of atmospheric hydroxyl radicals, Atmos. Meas. Tech., 7, 3413-3430, 2014.

Novelli, A., Hens, K., Tatum Ernest, C., Martinez, M., Nölscher, A. C., Sinha, V., Paasonen, P., Petäjä, T., Sipilä, M., Elste, T., Plass-Dülmer, C., Phillips, G. J., Kubistin, D., Williams, J., Vereecken, L., Lelieveld, J., and Harder, H.: Estimating the Atmospheric Concentration of Criegee Intermediates and Their Possible Interference in a FAGE-LIF Instrument, Atmos. Chem. Phys., 17, 7807-7826, 2017.

Peeters, J., Nguyen, T. L., and Vereecken, L.: $HO_x$ Radical Regeneration in the Oxidation of Isoprene, Phys. Chem. Chem. Phys., 11, 5935, 2009.

Peeters, J., Müller, J.-F., Stavrakou, T., and Nguyen, V. S.: Hydroxyl Radical Recycling in Isoprene Oxidation Driven by Hydrogen Bonding and Hydrogen Tunneling: The Upgraded LIM1 Mechanism, J. Phys. Chem. A, 118, 8625-8643, 2014.

Reidy, E., Rosales, C., Bottorff, B., Stevens, P. S., Cantrell, C. A., Mauldin, L. Anderson, D. C., and Wood, E. C. D. An Informal Intercomparison of Ambient OH, $HO_2$, and $RO_2$ Measurements in an Indiana Forest Part 2: Comparison with Model Predictions, Abstract A43M-3281 presented at 2018 Fall Meeting, AGU, Washington, D.C., 10-14 Dec., 2018.

Ren, X., Harder, H., Martinez, M., Lesher, R. L., Oliger, A., Simpas, J. B., Brune, W. H., Schwab, J. J., Demerjian, K. L., He, Y., Zhou, X., and Gao, H.: OH and $HO_2$ Chemistry in the Urban Atmosphere of New York City, Atmospheric Environment, 37, 3639-3651, 2003.

Ren, X., Brune, W., Cantrell, C., Edwards, G., Shirley, T., Metcalf, A., and Lesher, R.: Hydroxyl and Peroxy Radical Chemistry in a Rural Area of Central Pennsylvania: Observations and Model Comparisons, J. Atmos. Chem., 52, 231-257, 2005.

Ren, X., Brune, W. H., Oliger, A., Metcalf, A. R., Simpas, J. B., Shirley, T., Schwab, J. J., Bai, C., Roychowdhury, U., Li, Y., Cai, C., Demerjian, K. L., He, Y., Zhou, X., Gao, H., and Hou, J.: OH, $HO_2$, and OH Reactivity During the PMTACS-NY Whiteface Mountain 2002 Campaign: Observations and Model Comparison, J. Geophys. Res., 111, doi:10.1029/2005JD006126, 2006.

Ren, X., van Duin, D., Cazorla, M., Chen, S., Mao, J., Zhang, L., Brune, W. H., Flynn, J. H., Grossberg, N., Lefer, B. L., Rappenglück, B., Wong, K. W., Tsai, C., Stutz, J., Dibb, J. E., Thomas Jobson, B., Luke,W. T., and Kelley, P.: Atmospheric oxidation chemistry and ozone production: Results from SHARP 2009 in Houston, Texas, J. Geophys. Res., 118, 5770–5780, 2013.

Rickly, P., and Stevens, P. S.: Measurements of the OH Radical Yield from the Ozonolysis of Biogenic Alkenes: A Potential Interference with Laser-Induced Fluorescence Measurements of Ambient OH, Atmos. Meas. Tech. 11,1-16, 2018.

Rohrer, F., Lu, K., Hofzumahaus, A., Bohn, B., Brauers, T., Chang, C.-C., Fuchs, H., Haseler, R., Holland, F., Hu, M., Kita, K., Kondo, Y., Li, X., Lou, S., Oebel, A., Shao, M., Zeng, L., Zhu, T., Zhang, Y., and Wahner, A.: Maximum Efficiency in the Hydroxyl-Radical-Based Self-Cleansing of the Troposphere, Nature Geosci, 7, 559-563, 2014.

Rosales, C., Reidy, E., Bottorff, B., Stevens, P. S., Cantrell, C. A., Mauldin, L. Anderson, D. C., and Wood, E. C. D., An Informal Intercomparison of Ambient Measurements of OH, $HO_2$, and $RO_2$ Radicals in an Indiana Forest, Part 1: Comparison of Instrumental Measurements, Abstract A43M-3280 presented at 2018 Fall Meeting, AGU, Washington, D.C., 10-14 Dec., 2018.

Roukos, J., Plaisance, H., Leonardis, T., Bates, M., and Locoge, N.: Development and validation of an automated monitoring system for oxygenated volatile organic compounds and nitrile compounds in ambient air, J. Chromatr. A, 1216, 8642–8651, 2009.

Saunders, S. M., Jenkin, M. E., Derwent, R. G., and Pilling, M. J.: Protocol for the development of the Master Chemical Mechanism, MCM v3 (Part A): Tropospheric degradation of non-aromatic volatile organic compounds, Atmos. Chem. Phys., 3, 161-180, 2003.

Sheehy, P. M., Volkamer, R., Molina, L. T., and Molina, M. J.: Oxidative Capacity of the Mexico City Atmosphere – Part 2: A $RO_x$ Radical Cycling Perspective, Atmos. Chem. Phys., 10, 6993-7008, 2010.

Shetter, R. E., and M. Muller, Photolysis frequency measurements using actinic flux spectroradiometry during the PEM-Tropics mission: Instrumentation description and some results, J. Geophys. Res., 104, 5647–5661, doi:10.1029/98JD01381, 1999.

Shirley, T. R., Brune, W. H., Ren, X., Mao, J., Lesher, R., Cardenas, B., Volkamer, R., Molina, L. T., Molina, M. J., Lamb, B., Velasco, E., Jobson, T., and Alexander, M.: Atmospheric Oxidation in the Mexico City Metropolitan Area (MCMA) During April 2003, Atmos. Chem. Phys., 6, 2753-2765, 2006.

Sklaveniti, S., Locoge, N., Stevens, P. S., Wood, E., Kundu, S., and Dusanter, S.: Development of an instrument for direct ozone production rate measurements: measurement reliability and current limitations, Atmos. Meas. Tech., 11, 741-761, 2018.

Stevens, P. S., Mather, J. H., and Brune, W. H.: Measurement of Tropospheric OH and $HO_2$ by Laser-Induced Fluorescence at Low Pressure, J. Geophys. Res., 99, 3543-3557, 10.1029/93jd03342, 1994.

Tan, D., Faloona, I., Simpas, J. B., Brune, W., Shepson, P. B., Couch, T. L., Sumner, A. L., Carroll, M. A., Thornberry, T., Apel, E., Riemer, D., and Stockwell, W.: HOx Budgets in a Deciduous Forest: Results from the PROPHET Summer 1998 Campaign, J. Geophys. Res., 106, 24407-24427, 10.1029/2001jd900016, 2001.

Tan, Z., Fuchs, H., Lu, K., Hofzumahaus, A., Bohn, B., Broch, S., Dong, H., Gomm, S., Häseler, R., He, L., Holland, F., Li, X., Liu, Y., Lu, S., Rohrer, F., Shao, M., Wang, B., Wang, M., Wu, Y., Zeng, L., Zhang, Y., and Wahner, A.: Radical Chemistry at a Rural Site (Wangdu) in the North China Plain: Observation and Model Calculations of OH, $HO_2$ and $RO_2$ Radicals, Atmos. Chem. Phys., 17, 663-690, 2017.

Tan, Z., Rohrer, F., Lu, K., Ma, X., Bohn, B., Broch, S., Dong, H., Fuchs, H., Gkatzelis, G. I., Hofzumahaus, A., Holland, F., Li, X., Liu, Y., Liu, Y., Novelli, A., Shao, M., Wang, H., Wu, Y., Zeng, L., Hu, M., Kiendler-Scharr, A., Wahner, A., and Zhang, Y.: Wintertime photochemistry in Beijing: observations of $RO_x$ radical concentrations in the North China Plain during the BEST-ONE campaign, Atmos. Chem. Phys., 18, 12391–12411, 2018.

Tan, Z., Lu, K., Hofzumahaus, A., Fuchs, H., Bohn, B., Holland, F., Liu, Y., Rohrer, F., Shao, M., Sun, K., Wu, Y., Zeng, L., Zhang, Y., Zou, Q., Kiendler-Scharr, A., Wahner, A., and Zhang, Y.: Experimental budgets of OH, HO$_2$, and RO$_2$ radicals and implications for ozone formation in the Pearl River Delta in China 2014, Atmos. Chem. Phys., 19, 7129–7150, 2019.

Whalley, L. K., Edwards, P. M., Furneaux, K. L., Goddard, A., Ingham, T., Evans, M. J., Stone, D., Hopkins, J. R., Jones, C. E., Karunaharan, A., Lee, J. D., Lewis, A. C., Monks, P. S., Moller, S. J., and Heard, D. E.: Quantifying the Magnitude of a Missing Hydroxyl Radical Source in a Tropical Rainforest, Atmos. Chem. Phys., 11, 7223-7233, 2011.

Whalley, L. K., Blitz, M. A., Desservettaz, M., Seakins, P. W., and Heard, D. E.: Reporting the Sensitivity of Laser-Induced Fluorescence Instruments Used for HO$_2$ Detection to an Interference from RO$_2$ Radicals and Introducing a Novel Approach That Enables HO$_2$ and Certain RO$_2$ Types to Be Selectively Measured, Atmos. Meas. Tech., 6, 3425-3440, 2013.

Wolfe, G. M., Marvin, M. R., Roberts, S. J., Travis, K. R., and Liao, J.: The Framework for 0-D Atmospheric Modeling (F0AM) V3.1, Geosci. Model Dev., 9, 3309-3319, 2016.

Zannoni, N., Gros, V., Lanza, M., Sarda, R., Bonsang, B., Kalogridis, C., Preunkert, S., Legrand, M., Jambert, C., Boissard, C., and Lathiere, J.: OH reactivity and concentrations of biogenic volatile organic compounds in a Mediterranean forest of downy oak trees, Atmos. Chem. Phys., 16, 1619-1636, 2016.

Zhou, X., N. Zhang, M. TerAvest, D. Tang, J. Hou, S. Bertman, M. Alaghmand, P. B. Shepson, M. A. Carroll, S. Griffith, S. Dusanter and P. S. Stevens: Nitric acid photolysis on forest canopy surface as a source for tropospheric nitrous acid. Nature Geosci., 4, 440-443, 2011.

**Table 1: Measurements conducted during the IRRONIC field campaign.**

| Measurement | Instrument | Technique | LOD | Reference |
|---|---|---|---|---|
| OH | LIF-FAGE | Laser-induced fluorescence – fluorescence assay by gas expansion | $8 \times 10^5$ cm$^{-3}$ / 30 min | Dusanter et al., 2009a; Lew et al., 2018 |
| HO$_2$* | | | $7 \times 10^7$ cm$^{-3}$ / 20 s | |
| NO | Thermo 42i-TL | Chemiluminescence | 50 ppt / 2 min | |
| NO$_2$ | Aerodyne CAPS | Cavity attenuated phase shift spectroscopy | 40 ppt / 10 s | |
| Ozone | 2B Technologies Model 202 | UV absorbance | 3 ppb / 10 s | |
| OH reactivity | LIF-TOHLM | Total OH Loss Measurement | 1 s$^{-1}$ (10 min) | Hansen et al., 2013 |
| HONO | LP LIF-FAGE | Laser-photofragmentation laser-induced fluorescence | 20 ppt (30 min) | Bottorff et al., in prep |
| NMHCs | Online GC/FID | Gas chromatography with flame ionization detection | 10-100 ppt (1.5 hr) | Badol et al., 2004 |
| OVOCs | Online GC/FID-MS | Gas chromatography with mass spectrometer and FID | 5-100 ppt (1.5 hr) | Roukos et al. (2009) |
| | Off-line Sorbent GC-MS | Sorbent cartridges analyzed by GC-MS | | Detournay et al. (2011); Ait-Helal et al. (2014) |
| | Off-line DNPH HPLC-UV | Dinitrophenylhydrazine cartridges analyzed by high-performance liquid chromatography with UV detection | | |
| J(NO$_2$) | | Spectral Radiometry | $0.3 \times 10^{-4}$ s$^{-1}$ | Shetter and Muller (1999) |
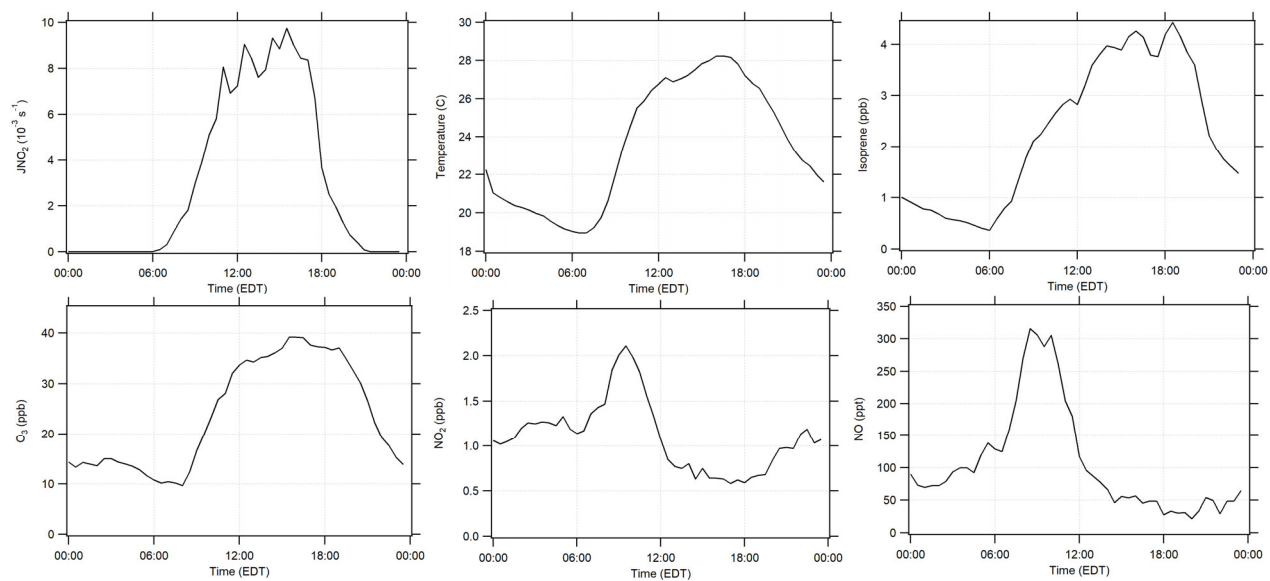
**Figure 1.** Diurnal campaign average profiles of J(NO$_2$), temperature, isoprene, O$_3$, NO$_2$, and NO.
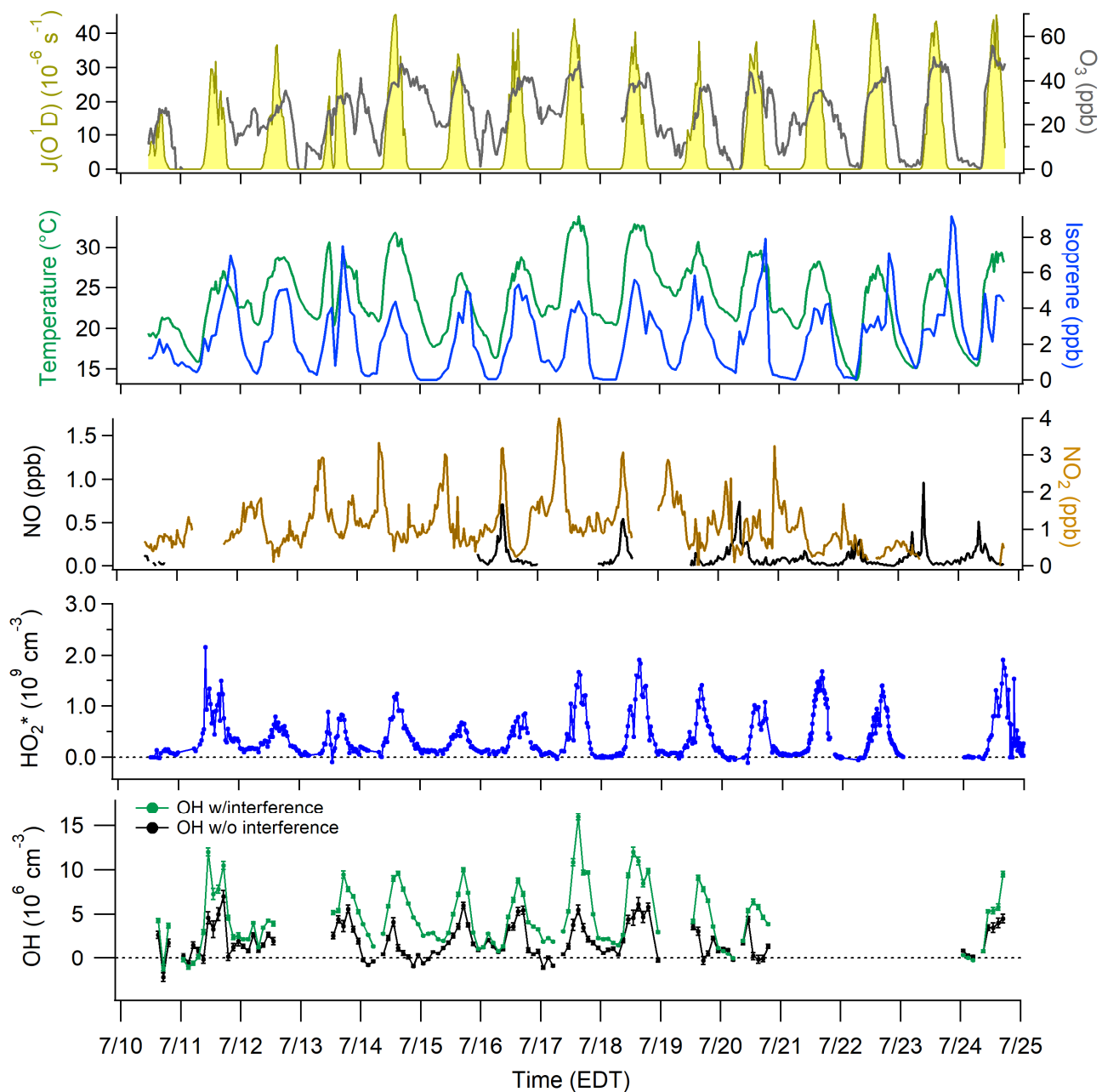
**Figure 2.** Time series of OH and HO$_2$* from July 10 to July 25 with model calculated J(O$^1$D) scaled to the measured J(NO$_2$), and measured ozone, temperature, isoprene, and NO$_x$. OH measurements with interference ($\pm$ 1$\sigma$) represented by the green line and measurements without interference ($\pm$ 1$\sigma$) represented by the black line. For clarity, OH data shown are 2 hour averages. HO$_2$* data are 30 s averages every 30 minutes.
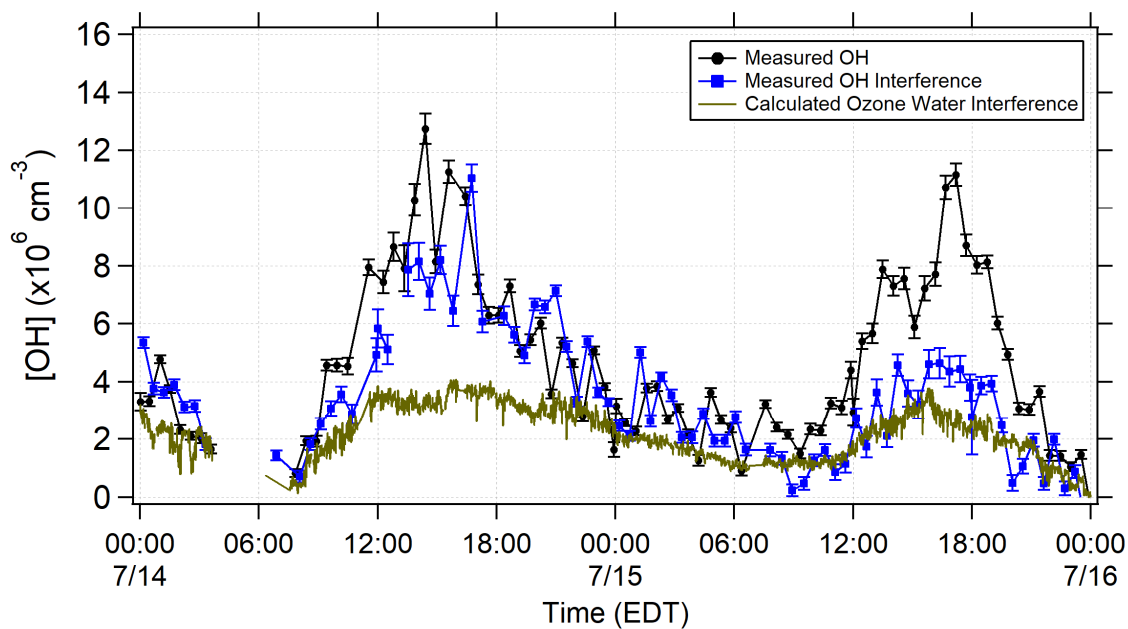
**Figure 3.** Averaged measured total OH signal using spectral modulation (black), and the measured interference using chemical modulation (blue) during July 14 and July 15. The calculated laser-generated interference from ozone photolysis for these days (reactions 1 and 2, green points) is also shown.
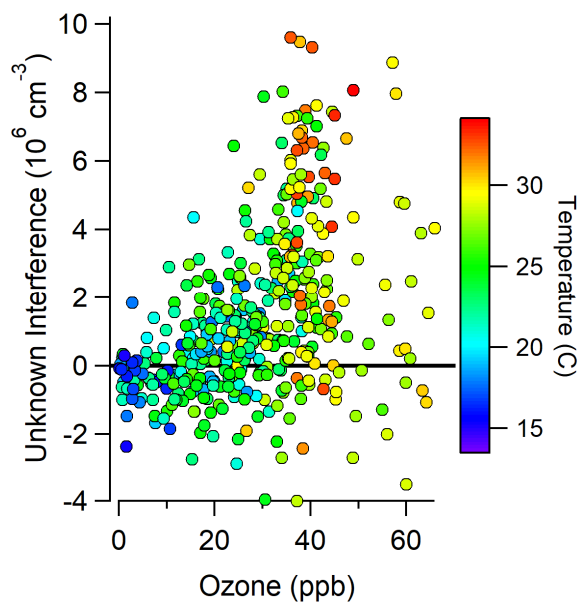


**Figure 4.** Measurements of the unknown interference as a function of ozone and temperature during the campaign.

30
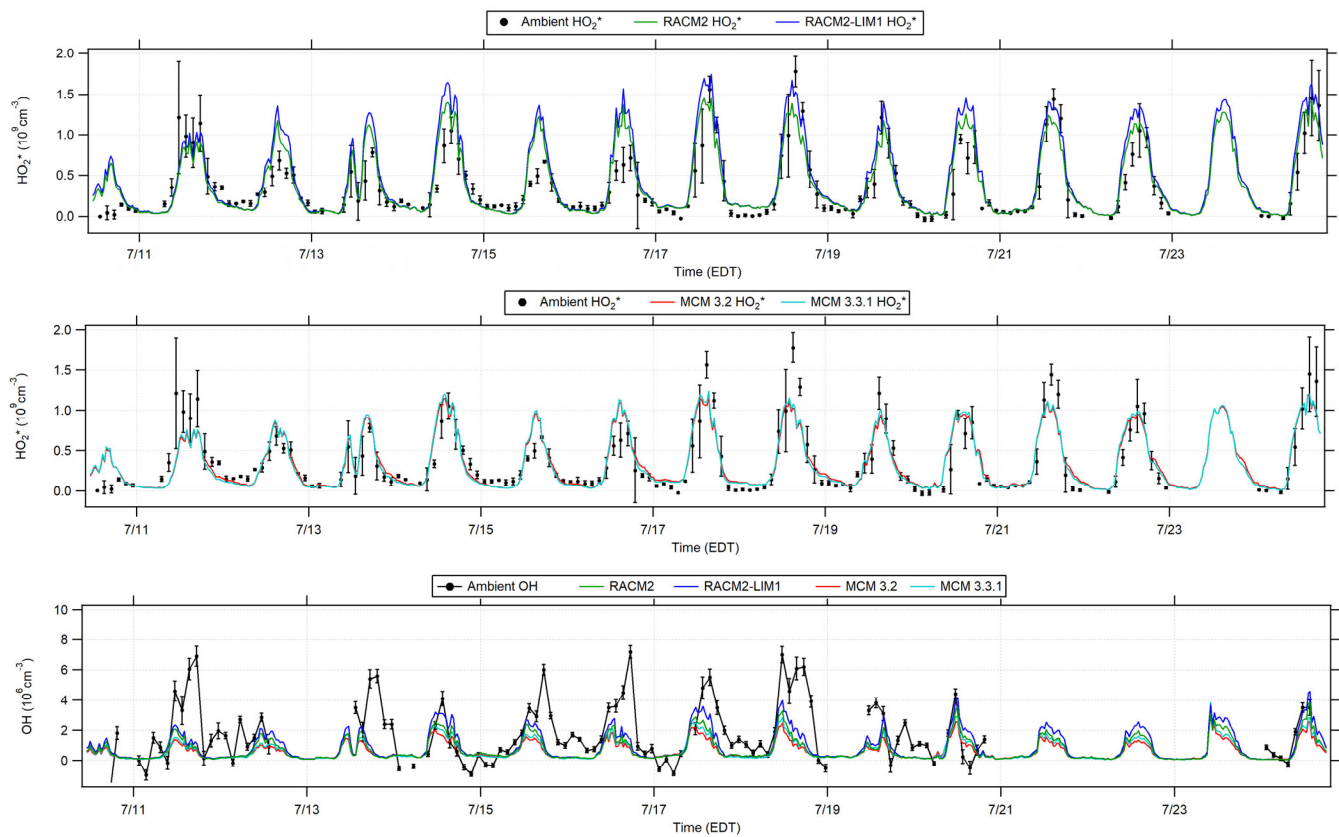
**Figure 5.** Average measurements of OH (bottom) and HO$_2$* from July 10 to July 25 during the IRRONIC campaign in comparison to modeled results for RACM2 and RACM2-LIM1 models (top) and the MCM 3.2 and MCM 3.3.1 models (middle). The error bars represent the precision of the measurements (1σ).

31
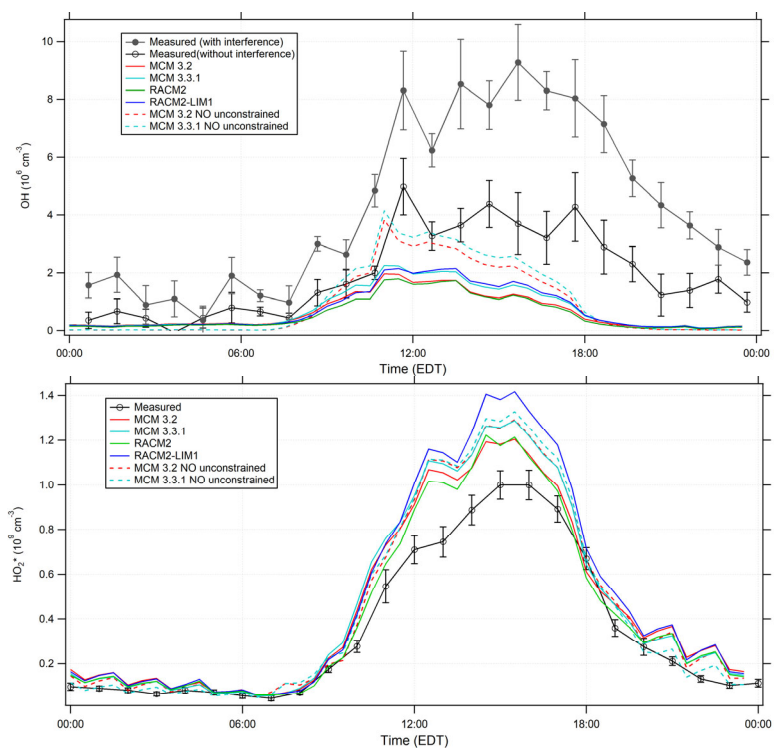
**Figure 6.** Diurnal profiles of OH (top) and HO$_2$* (bottom) with the RACM2, RACM2-LIM1, MCM 3.2, and MCM 3.3.1 model results. The open circles represent the 1 hour mean ± 1σ standard error of OH and HO$_2$* measurements. The filled circles represent the 1 hour mean ± 1σ standard error of the OH measurements with the interference. The dashed lines represent the MCM 3.2 and 3.3.1 model results with NO concentrations unconstrained (see text).

32
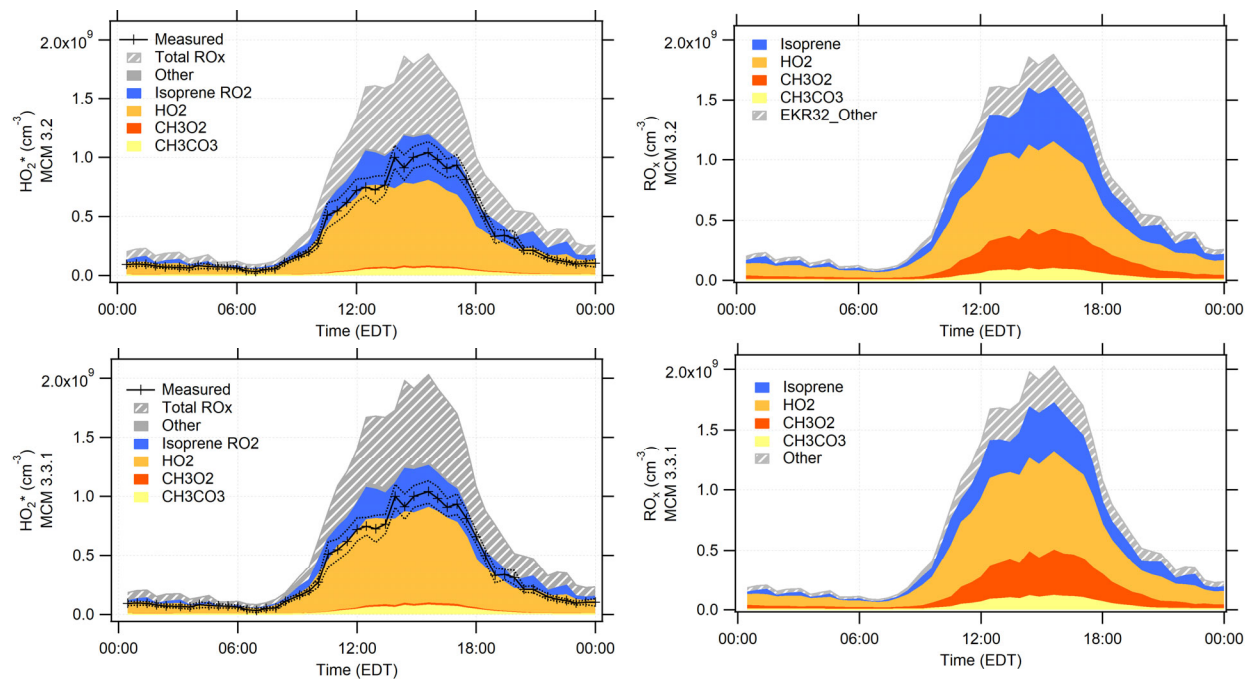
**Figure 7.** The MCM 3.2, and MCM 3.3.1 diurnal average modeled peroxy radical concentration and composition. Left panels show the modeled contribution to the measured $HO_2^*$ concentrations. The measured 30-min mean $HO_2^*$ concentrations are shown by the black line with $\pm 1\sigma$ standard error shown by the dotted lines. Right panels show the total $RO_x$ ($RO_2 + HO_2$) composition predicted by each model.
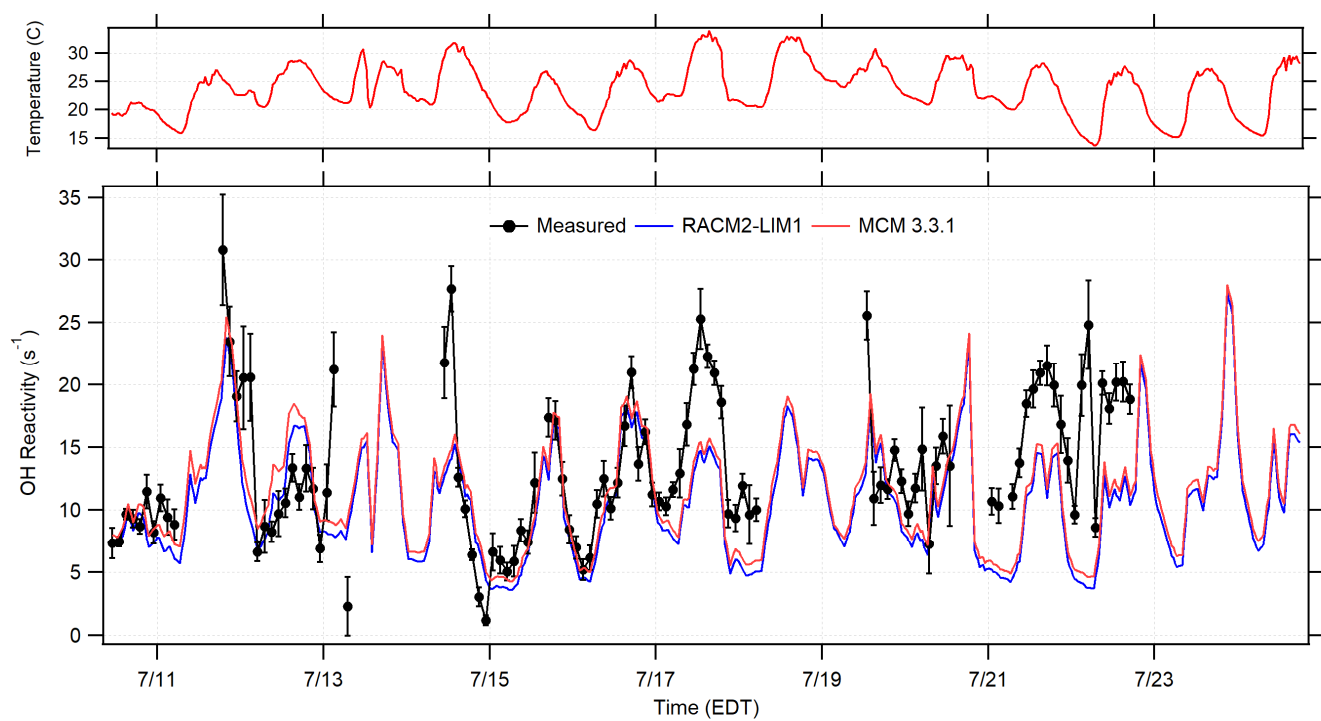
**Figure 8.** Time series of the 2 hour averaged OH reactivity measurements (black circles) in comparison to the RACM2-LIM1 and MCM 3.3.1 calculated OH reactivity based on measured OH sinks along with ambient temperature (top). Error bars represent the standard error of the average measurement.
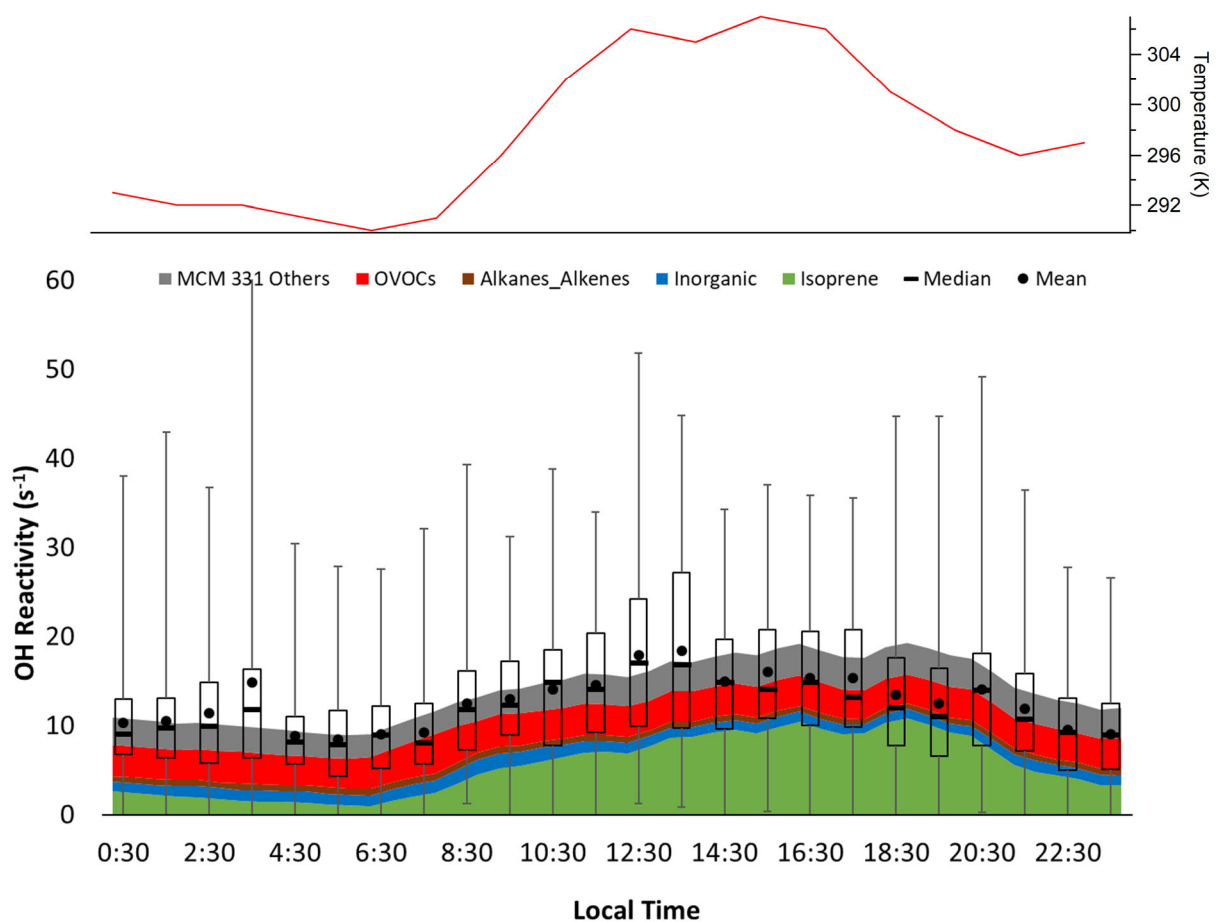
**Figure 9.** Diurnal temperature (top) and box and whiskers plot of observed total OH reactivity showing the mean and median values for each hour, with the mean calculated values from the measured OH sinks as well as the unmeasured oxidation products from the MCM 3.3.1 model results (Others). Error bars show the range of individual 5-min measurements and bars show Q1 and Q3 for the measured OH reactivity.
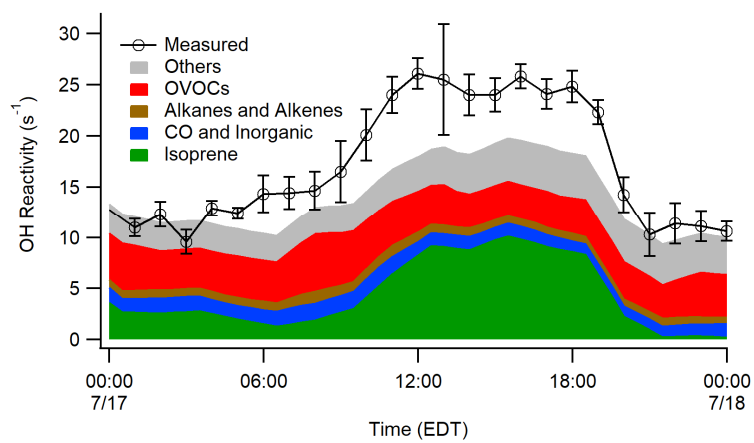
**Figure 10.** Median diurnally averaged OH reactivity from July 17 in comparison to modeled reactivity from the MCM 3.3.1 mechanism.
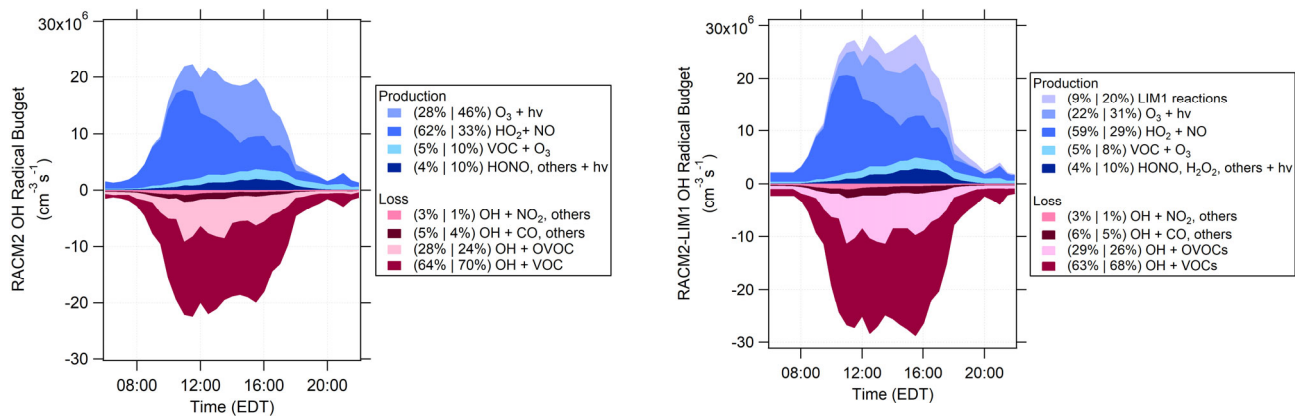
**Figure 11.** RACM2 (left) and RACM2-LIM1 (right) OH radical budgets where the shades of blue represent production reactions and the shades of red represent loss rates. The percent contribution of each reaction to total production/loss are divided into two periods (10:00 to 14:00 and 14:00 to 18:00).
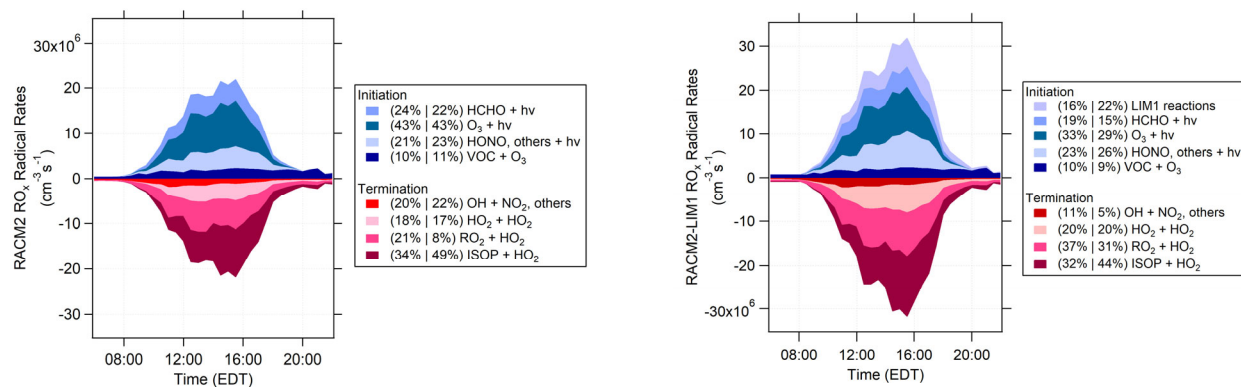


**Figure 12.** RACM2 (left) and RACM2-LIM1 (right) total $RO_x$ radical budgets where the shades of blue represent initiation rates and the shades of red represent termination rates. The percent contribution of each reaction to total initiation/termination are divided into two periods (10:00 to 14:00 and 14:00 to 18:00).